Engineering Analysis with Boundary Elements 83 (2017) 1–24

Contents lists available at ScienceDirect

Engineering Analysis with Boundary Elements

journal homepage: www.elsevier.com/locate/enganabound

Efficient analysis of plates on nonlinear foundations

Ahmed Fady Farid [a], Marina Reda [a], Youssef F. Rashed [a,b,*]

[a] Department of Structural Engineering, Cairo University, Giza, Egypt
[b] Supreme Council of Universities in Egypt, Egypt

ARTICLE INFO

Keywords:
Boundary element method
Finite element method
Iterative solution
Tensionless
Elastic-plastic
Plates

ABSTRACT

This paper presents efficient analysis of plates on nonlinear foundations. The Reissner plate theory is used to model plates. Foundations are presented as the Winkler springs or the elastic half space. The developed analysis is mainly presented for tensionless foundation; however as demonstrated, it is straightforward extended to analysis of elastic-plastic foundations. The plate is analyzed using the boundary element method (BEM). Unlike the traditional BEM which uses equations in form ([H] {u} = [G] {t}), the presented formulation uses finite element like equations, in the form of ([K] {u} = {P}). An innovative formulation is presented to derive the relevant plate stiffness matrix [K] and load vector {P} from the BEM integral equation. Iterative procedures together with condensation process are used to eliminate degree of freedom at failed zones. Results of the present analysis are more accurate than those obtained from previously published results. The main advantages of the presented technique are its simplicity and accuracy and it gains both advantages of the boundary element and the finite element methods.

1. Introduction

Plates on nonlinear (tensionless or elastic-plastic) foundations are an important problem in mechanics and have several applications in practical structural and geotechnical engineering. Numerical analysis of plates over elastic foundations (Winkler springs or elastic half space) is considered by many authors as follows:

(a) Using the finite element method: the work of Cheung and Zienkiewicz [2], Svec and McNeice [3], Svec and Gladwel [4] for thin plates, Rajapaks and Selvadurai [6] for thick plates.
(b) Using the boundary element method: the work of Katsikadelis and Armenakas [5], Syngellakis and Bai [7], Paiva and Butterfield [8] for thin plates, Rashed et al. [9–12] for thick plates.

Solving plates on tensionless foundation can be categorized into two main categories. The first category involves solution using iterative procedure to consider the miscontact between plate and foundation. The second category, on the other hand, involves solution by transforming the problem into a set of nonlinear equations, which could be solved using optimization algorithms.

Among the previous literature which follows the first category are: the work of Cheung and Nag [13] who presented a finite element analysis of beams and plates on linear and nonlinear elastic continuum. Weitsman [14] presented an approximate solution for the radius of contact between an elastic plate and a semi-infinite elastic half space subjected to concentrated load. Weitsman [15] presented analysis of tensionless beams, or plates, and their supporting Winkler or Reissner foundations due to concentrated loads. Svec [16] developed a finite element iterative procedure to determine the contact region between the plate and the elastic half space. The continuous contact pressure is approximated in [16] by a set of statically equivalent forces acting at the nodal points of the elements. Hence, the plate could be considered to be resting on a complicated system of springs. Celep [17] presented the behavior of elastic plates of rectangular shape on a tensionless Winkler foundation using auxiliary function. Galerkin's method is used in [17] to reduce the problem to a system of algebraic equations. Li and Dempsey [18] used an iterative procedure to analyze unbonded contact of a square thin plate under centrally symmetric vertical loading on elastic Winkler or elastic half space foundations. Hu and Hartely [19] solved thin plate on tensionless elastic half space using integral equations. Analysis using the T-element of plates on unilateral elastic Winkler type foundation is presented by Jirousek et al. [20]. Nonlinear bending behavior of Reissner–Mindlin plates with free edges resting on tensionless elastic foundations of the Pasternak-type using admissible functions is presented by Hui-Shen and Yu [21]. Results of finite element analysis of beam elements on unilateral elastic foundation using special zero thickness element designed for foundation modeling is presented by Torbacki [22]. Buczkowski and Torbacki [23] presented finite element analysis of plate on layered tensionless foundation. Kongtng and Sukawat [24] used the method of finite Hankel integral transform to solve the mixed boundary value problem of unilaterally supported rectangular plates loaded by uniformly distributed load.

The studies based on the second category, on the other hand, could be listed as follows:

* Corresponding author at: Department of Structural Engineering, Cairo University, Giza, Egypt.
E-mail addresses: yrashed@scu.eg, yrashed@hotmail.com (Y.F. Rashed).

http://dx.doi.org/10.1016/j.enganabound.2017.07.003
Received 6 December 2016; Received in revised form 23 June 2017; Accepted 6 July 2017
0955-7997/

Sapountzakis and Katsikadelis [25] presented boundary element solution for unilateral contact problems of thin elastic plates resting on linear or nonlinear subgrade by solving a system of nonlinear algebraic equations. Xiao et al. [26] presented a coupled boundary element local complementary equation method (BE-LCEM) to solve thin free edge plates on elastic half space with unilateral contact. Silva et al. [27] used the finite element method to discretize the plate and foundation. Hence they used three alternative optimization techniques to solve plates on tensionless elastic foundations. Xiao [28] presented a BE-LCEM solution to solve unilateral free edges thick plates. Nonlinear analysis of structural elements under unilateral contact constrains studied via Ritz approach using mathematical programming technique is presented by Silveira et al. [29].

Among the previous literature review, the following three important works are re-considered herein in more details as they will be considered for the sake of comparison in Section 6 in this paper:

(1) The work of Hu and Hartely [19] in 1994:
They used the boundary element method to solve thin plates on tensionless elastic half space. In their formulation the flexibility equations obtained from the BEM ([H] {u} = [G] {t}) is directly coupled to the flexibility equations of the elastic half space. Unilateral contact between plate and elastic half space is solved using iterations by eliminating the tensile stress values. This was carried out by removing the row and column of the flexibility matrix that corresponds to the relevant DOF. It has to be noted that this removal operation is suitable for flexibility-like equations; however, as will be demonstrated in this paper (Section 3), this elimination procedure is carried out using condensation which is suitable for stiffness-like equations ([K] {u} = {P}). In addition Hu and Hartely formulation in Ref. [19] demonstrated difficulty in computing bending moments in vicinities of concentrated loads, which will not be the case in the presented formulation.

(2) The work of Silva et al. [27] in 2001:
Silva et al. [27] used the finite element method to solve thin or thick plates on tensionless foundations via optimization algorithms. They presented only one example that solves plate on tensionless elastic half space. This example was previously solved in Hu and Hartely [19]. Only displacements along centerline were compared and no bending moments results were reported. This example will be presented in Section 6.4 for the purpose of comparison.

(3) The work of Xiao [28] in 2001:
Xiao [28] solved unilateral free edges thick plates using the boundary element method. He presented the fundamental solution in terms of two Hu's potential functions. This leads to have high order singularities in his formulation; therefore he used a regular collocation scheme to avoid treatment of singularities that appeared in his formulation. It will be demonstrated in Sections 6.3 and 6.5 in this paper this leads to loose of accuracy near corners.

As previously demonstrated the available examples that consider solution of the plates on elastic half space considering nonlinearities is rare. However, there are few available finite element based software packages that could model half space as 3D solid elements. Despite the huge computational cost for such models, they give somehow good representation of the half space. Moreover such models are feasible for small test cases; therefore in Section 6.5 in this paper such a model is used to compare contact zones, deflections, foundation pressures and bending moments.

Generally, in this paper an iterative procedure (follows the first category) is developed to solve thick plates (as a more general theory that can model thin and thick plates [9–12]) on tensionless Winkler or elastic half space foundation. The boundary element method is used, in an innovative way, to extract the stiffness matrix and the load vector of the plate. The Mindlin's equations [30] are used to compute the elastic half space stiffness matrix. A coupling technique is used to assembly the overall stiffness matrix and load vector of the problem. The main advantage of the proposed technique is it inherits advantages of the boundary element method in modeling plate using integral equation and the simplicity of finite element like procedures in the coupling between plate and foundation. The proposed technique is simple, practical and it is suitable to be extended to include elastic-plastic analysis as will be presented in this paper (Section 4). Numerical examples are presented to verify the efficiency and practicality of the proposed technique.

2. Proposed boundary elements for plate on elastic foundation

In this section, the direct boundary element formulation of thick plates is reviewed. Hence an innovative derivation of plate stiffness matrix and load vector is presented. Finally a coupling technique between the plate and the foundation stiffness matrices is presented.

2.1. Boundary element for plates

Consider a general thick plate [1] of domain Ω and boundary Γ with internal stiffness cells as shown in Fig. 1. The stiffness cells are defined as supporting cells such as supporting columns, walls, piles, or foundation reactions. Each stiffness cell has three unknown reactions (two moments and one shear). The indicial notation is used in this paper where the Greek indexes vary from 1 to 2 and Roman indexes vary from 1 to 3. The relevant integral equation can be rewritten as follows [11]:

$$
\begin{aligned}
C_{ij}(\xi)\, u_j(\xi) &+ \int_{\Gamma(x)} T_{ij}(\xi, x)\, u_j(x) d\Gamma(x) = \int_{\Gamma(x)} U_{ij}(\xi, x)\, t_j(x) d\Gamma(x) \\
&+ \int_{\Gamma(x)} \left[V_{i,n}(\xi, x) - \frac{\nu}{(1-\nu)\lambda^2} U_{i\alpha}(\xi, x) n_\alpha(x) \right] q_3(x) d\Gamma(x) \\
&+ \sum_{N_q} \int_{\Omega(L)} \left[U_{ik}(\xi, L) - \frac{\nu}{(1-\nu)\lambda^2} U_{i\alpha,\alpha}(\xi, L) \delta_{3k} \right] P_k(L) d\Omega(L) \\
&+ \sum_{N_{sc}} \int_{\Omega(y)} \left[U_{im}(\xi, y) - \frac{\nu}{(1-\nu)\lambda^2} U_{i\alpha,\alpha}(\xi, y) \delta_{3m} \right] F_m(y)\, d\Omega(y)
\end{aligned}
\tag{1}
$$

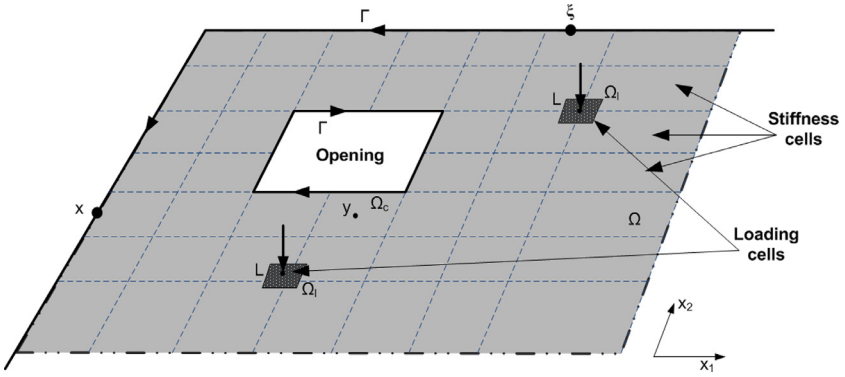

Fig. 1. Plate geometry and definitions.

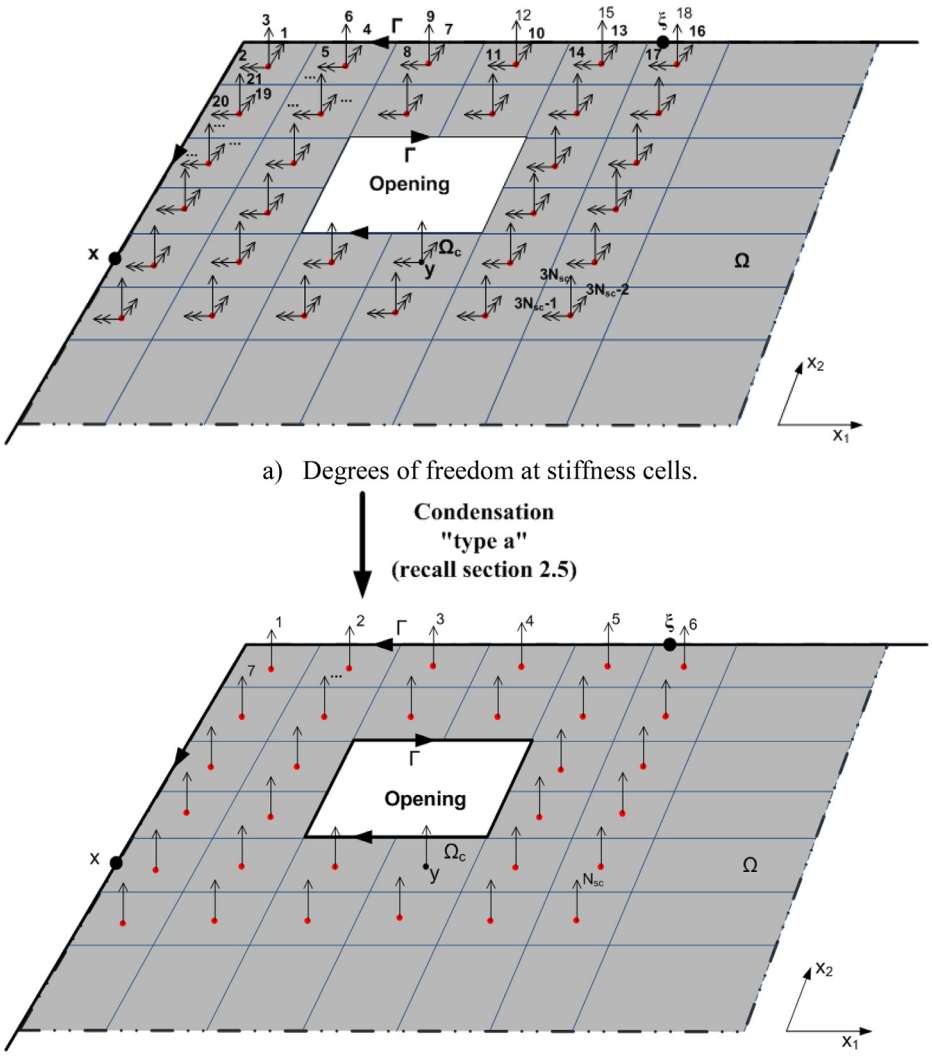

Fig. 2. Condensation procedure of postulated degrees of freedom.

where $T_{ij}(\xi,x)$, $U_{ij}(\xi,x)$ are the two-point fundamental solution kernels for tractions and displacements respectively [11]. The two points ξ and x are the source and the field points respectively. $u_j(x)$ and $t_j(x)$ denote the generalized boundary displacements and tractions. $C_{ij}(\xi)$ is the jump term. $V_i(\xi,x)$ is a suitable particular solutions to represent domain loading [11]. The symbols ν and λ denote the plate Poison's ratio and shear factor. $q_3(x)$ denotes the intensity of domain loading. N_q denotes the number of loading cells (such as applied column or wall loads) that having domain Ω_L, P_k denotes the three load cases for loading cell (two moments and one shear). The field point L denotes the loading cell center. N_{sc} denotes the number of internal stiffness cells that having domain Ω_c, F_m denotes the three unknown forces for stiffness cells. The field point y denotes the point of the internal stiffness cell center. It has to be noted that, in this paper, all used domain cells are of constant type. After discretizing the boundary of the plate to N_e quadratic elements (without losing the generality, any boundary element could be used), each node has three unknowns. Eq. (1) can be re-written in a matrix form as follows:

$$
\begin{array}{c}
\begin{array}{ccc} & 3N & 3N_{sc} \end{array} \\
3N \begin{bmatrix} C_{ij}(\xi)\, u_j(\xi) \\ + \\ \int_{\Gamma(x)} T_{ij}(\xi,x) \\ \text{or} \\ -\int_{\Gamma(x)} U_{ij}(\xi,x) \\ \text{Corresponding to unknowns boundary values} \end{bmatrix} \begin{bmatrix} \int_{\Omega(y)} U_{im}(\xi,y) \end{bmatrix}
\end{array}
\times
\begin{array}{c}
\begin{array}{c} 1 \end{array} \\
\begin{bmatrix} \{u_j(x)\} \\ \text{or} \\ \{t_j(x)\} \end{bmatrix} \\
3N_{sc} \begin{bmatrix} \{F(y)\} \end{bmatrix}
\end{array}
=
\begin{array}{c}
\begin{array}{c} 1 \end{array} \\
3N \begin{bmatrix} \{LF\} \\ - \\ \{PBIV\} \end{bmatrix}
\end{array}
\qquad (2)
$$

where, N is the number of nodes. The vector $\{LF\}_{3N\times 1}$ contains domain loading and patch loading effects. The vector $\{PBIV\}_{3N\times 1}$ contains prescribed boundary integral values. The vector $\{F(y)\}_{3Nsc\times 1}$ contains the unknown values of internal stiffness cell forces. It can be seen that Eq. (2) contains additional three unknowns at each internal stiffness cell. Therefore, another collocation scheme should be carried out at each internal stiffness cell center to add additional equations, as follows:

	3N	$3N_{sc}$	$3N_{sc}$		1		1
3N	$C_{ij}(\xi)\,u_j(\xi) + \int_{\Gamma(x)} T_{ij}(\xi,x)$ Or $-\int_{\Gamma(x)} U_{ij}(\xi,x)$ Corresponding to unknowns boundary values	$\int_{\Omega(y)} U_{im}(\xi,y)$	[0]	3N	$\{u_j(x)\}$ or $\{t_j(x)\}$	3N	$\{LF\} - \{PBIV\}$
$3N_{sc}$	$\int_{\Gamma(x)} T_{ij}(Y,x)$ or $-\int_{\Gamma(x)} U_{ij}(Y,x)$ Corresponding to unknowns stiffness cells values	$\int_{\Omega(y)} U_{im}(Y,y)$	[I]	$3N_{sc}$	$\{F(y)\}$	$3N_{sc}$	$\{LF2\}$
				$3N_{sc}$	$\{u(y)\}$		

(4)

where, Y is a new source point located at each stiffness cell center. Using Eqs. (1) and (3), Eq. (2) could be re-written in matrix form, as follows:

where, the vector $\{LF2\}_{3Nsc\times 1}$ contains domain loading and patch loading effects due to the second collocation scheme in Eq. (3). The vector $\{u(y)\}_{3Nsc\times 1}$ contains the unknown values of the generalized displacements at internal stiffness cells.

Eq. (4) could be re-written as follows:

	3N	$3N_{sc}$		1		1
3N	$C_{ij}(\xi)\,u_j(\xi) + \int_{\Gamma(x)} T_{ij}(\xi,x)$ or $-\int_{\Gamma(x)} U_{ij}(\xi,x)$ Corresponding to unknowns boundary values	$\int_{\Omega(y)} U_{im}(\xi,y)$	3N	$\{u_j(x)\}$ or $\{t_j(x)\}$	3N	$\{LF\} - \{PBIV\}$
$3N_{sc}$	$\int_{\Gamma(x)} T_{ij}(Y,x)$ or $-\int_{\Gamma(x)} U_{ij}(Y,x)$ Corresponding to unknowns stiffness cells values	$\int_{\Omega(y)} U_{im}(Y,y)$	$3N_{sc}$	$\{F(y)\}$	$3N_{sc}$	$\{LF2\} - \{u(y)\}$

(5)

It can be seen the new matrix form in Eq. (5) contains direct relationship between the displacements {u(y)} and the corresponding forces {F(y)} at internal stiffness cells. In the next two subsections, such a relationship will be employed to derive a suitable stiffness matrix and load vector for the considered plate.

2.2. Innovative derivation of plate stiffness matrix

Eq. (5) could be used to extract the stiffness matrix of the plate at degrees of freedom postulated at domain stiffness cells; as shown in Fig. 2a. It has to be noted that each cell has two rotational degrees of

$$
\begin{aligned}
u_i(Y) + \int_{\Gamma(x)} T_{ij}(Y,x)\,u_j(x)d\Gamma(x) &= \int_{\Gamma(x)} U_{ij}(Y,x)\,t_j(x)d\Gamma(x) \\
&+ \int_{\Gamma(x)} \left[V_{i,n}(Y,x) - \frac{\nu}{(1-\nu)\lambda^2} U_{i\alpha}(Y,x)n_\alpha(x)\right] q_3(x)d\Gamma(x) \\
&+ \sum_{N_q} \int_{\Omega(L)} \left[U_{ik}(Y,L) - \frac{\nu}{(1-\nu)\lambda^2} U_{i\alpha,\alpha}(Y,L)\delta_{3k}\right] P_k(L)d\Omega(L) \\
&+ \sum_{N_{sc}} \int_{\Omega(y)} \left[U_{im}(Y,y) - \frac{\nu}{(1-\nu)\lambda^2} U_{i\alpha,\alpha}(Y,y)\delta_{3m}\right] F_m(y)\,d\Omega(y)
\end{aligned}
\tag{3}
$$

freedom and single displacement degree of freedom. Stiffness matrix of the plate is independent of loading; therefore no domain load or patch loading is considered; i.e. {LF} and {LF2} are set to zeros.

In order to force $\{F(y)\}_{3Nsc\ x\ 1}$ to represent the stiffness matrix, as $3N_{sc}$ cases of loading are considered. Each considered load case is set to have a unit generalized displacement in a single degree of freedom and zeros at the other degrees of freedom (recall the definition of the stiffness matrix). That means the vector $\{u(y)\}_{3Nsc\ x\ 1}$ is replaced by a matrix $[u(y)]_{3Nsc\ x\ 3Nsc}$ and such a matrix is forced to be the unity matrix ([I]), as follows:

$$\begin{array}{c|c|c|c|c} & 3N & 3N_{sc} & 3N_{sc} & 3N_{sc} \\ 3N & \begin{array}{l} C_{ij}(\xi)\,u_j(\xi) \\ + \\ \int_{\Gamma(x)} T_{ij}(\xi,x) \\ Or \\ -\int_{\Gamma(x)} U_{ij}(\xi,x) \\ \text{Corresponding to unknowns boundary values} \end{array} & \int_{\Omega(y)} U_{im}(\xi,y) & \begin{array}{l}\{u_j(x)\} \\ or \\ \{t_j(x)\}\end{array} & -[PBIV] \\ 3N_{sc} & \begin{array}{l} \int_{\Gamma(x)} T_{ij}(Y,x) \\ or \\ -\int_{\Gamma(x)} U_{ij}(Y,x) \\ \text{Corresponding to unknowns stiffness cells values} \end{array} & \int_{\Omega(y)} U_{im}(Y,y) & [K_P] & -[I] \end{array} \quad (6)$$

where $[K_p]_{3Nsc\ x\ 3Nsc}$ is the required plate stiffness matrix. It has to be noted that such a matrix is not symmetric. However, in this work a forcing of the symmetry is carried out by averaging the off-diagonal terms. It has seen from Eq. (6) that each column of the matrix [PBIV] represents the values of the known boundary displacements $\{u_j\}$ and tractions $\{t_j\}$ corresponding to the associated stiffness cases (i.e. corresponding to a unit displacement at a certain degree of freedom). This matrix is used in Section 5 for the purpose of post-processing.

2.3. Innovative derivation of plate load vector

Similar to the formulation presented in the previous subsection, Eq. (5) could be used to extract the load vector of the plate at relevant degrees of freedom. In this case, if all displacements at degrees of freedom are set to zero (i.e. $\{u(y)\} = \{0\}$), the corresponding $\{F(y)\}$ in Eq. (5) is the desired load vector $\{P\}$ due to the loading $\{LF\}$. This could be written as follows:

$$\begin{array}{c|c|c|c|c} & 3N & 3N_{sc} & 1 & 1 \\ 3N & \begin{array}{l} C_{ij}(\xi)\,u_j(\xi) \\ + \\ \int_{\Gamma(x)} T_{ij}(\xi,x) \\ or \\ -\int_{\Gamma(x)} U_{ij}(\xi,x) \\ \text{Corresponding to unknowns boundary values} \end{array} & \int_{\Omega(y)} U_{im}(\xi,y) & \begin{array}{l}\{u_j(x)\} \\ or \\ \{t_j(x)\}\end{array} & \begin{array}{l}\{LF\} \\ - \\ \{PBIV\}^1\end{array} \\ 3N_{sc} & \begin{array}{l} \int_{\Gamma(x)} T_{ij}(Y,x) \\ or \\ -\int_{\Gamma(x)} U_{ij}(Y,x) \\ \text{Corresponding to unknowns stiffness cells values} \end{array} & \int_{\Omega(y)} U_{im}(Y,y) & \{P\} & \{LF2\} \end{array} \quad (7)$$

It has to be noted that both Eqs. (6) and (7) could be solved simultaneously to obtain the desired stiffness matrix and load vector in one-step saving computational time.

2.4. Foundation stiffness

The underneath soil or the foundation is modeled as elastic half space (EHS) [12], where its boundary surface is discritized into a number of cells N_{cb} as shown in Fig. 3a. It has to be noted that, these discritization should match the plate domain discritization for the purpose of coupling. Using the elastic solution of Mindlin [30], the flexibility matrix of the foundation $[F_{Soil}]_{Ncb \times Ncb}$ is computed at center of each cell. Stiffness matrix of the EHS, $[K_{Soil}]_{Ncb \times Ncb}$ could be computed as its inverse. It has to be noted that; if the soil is modeled as Winkler springs, the stiffness matrix $[K_{Soil}]_{Ncb \times Ncb}$ in this case is a diagonal matrix.

2.5. Coupling plate and foundation

In order to couple the $[K_P]_{3Nsc \times 3Nsc}$ and $[K_{Soil}]_{Ncb \times Ncb}$, two types of degrees of freedom have to be eliminated, via static condensation procedures:

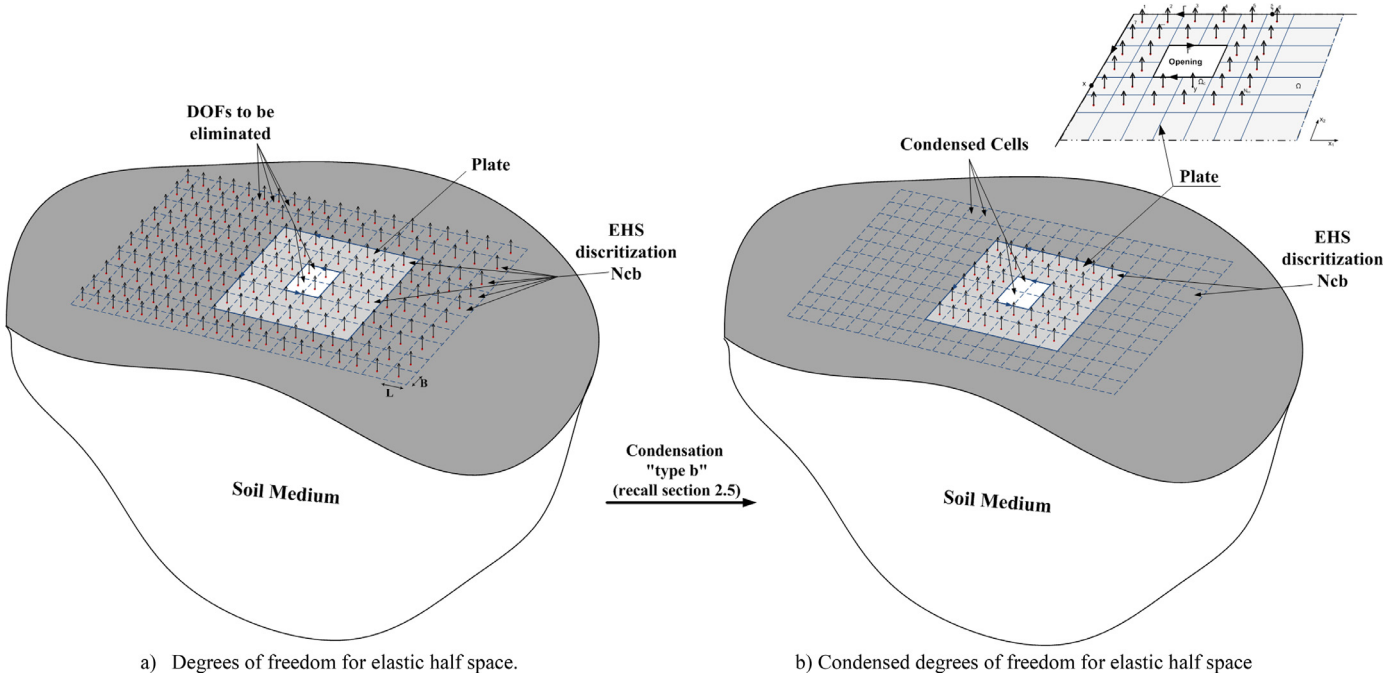

a) Degrees of freedom for elastic half space. b) Condensed degrees of freedom for elastic half space

Fig. 3. Coupling degrees of freedom between plate and elastic half space.

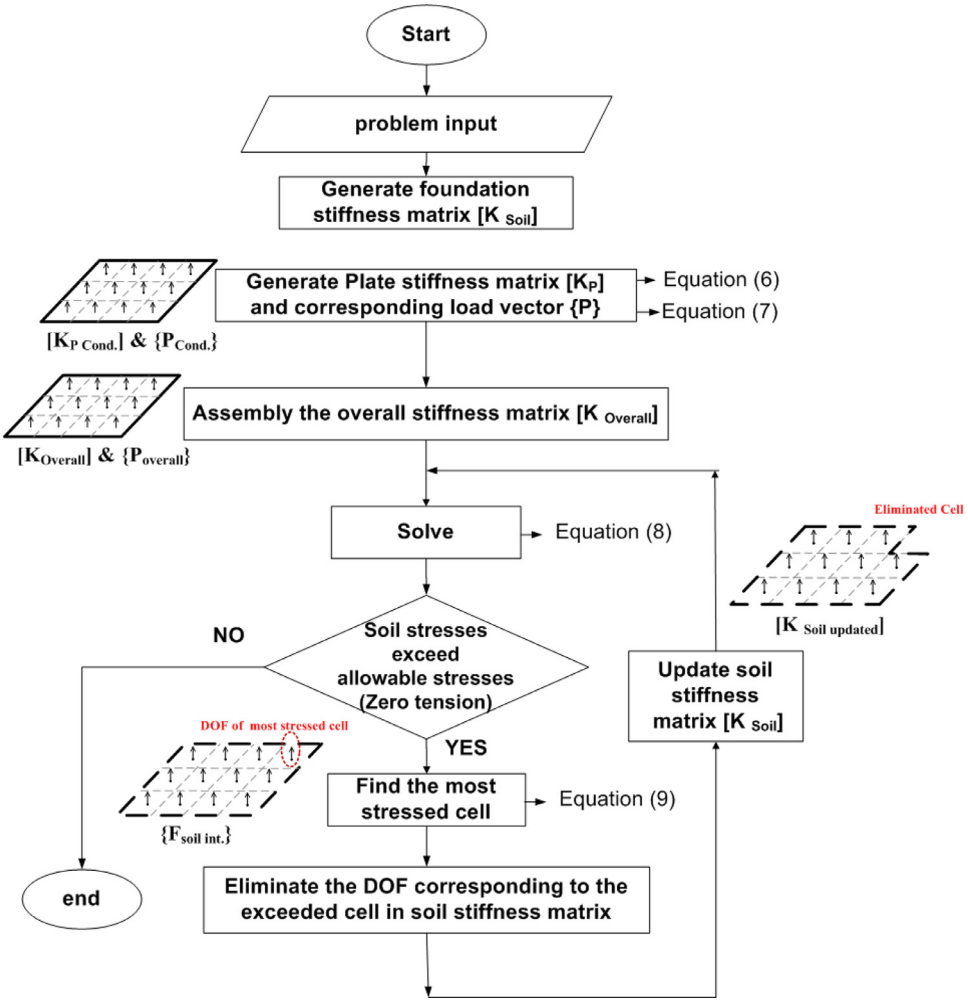

Fig. 4. Flowchart of the programmed technique.

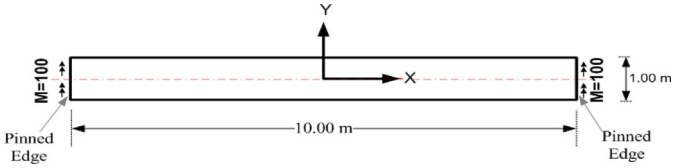

Fig. 5. The simply supported beam in example 1.

Type a: the plate rotational degrees of freedom in two directions as shown in Fig. 2b. Once performed, the plate stiffness matrix becomes of dimensions $[K_{Plate}]_{Nsc \times Nsc}$,

Type b: the foundation degrees of freedom which located outside the plate or inside the plate openings as shown in Fig. 3b. In other words, these DOFs are considered as dependent DOFs. After such a process, the foundation stiffness becomes of dimensions $[K_{Soil}]_{Nsc \times Nsc}$.

Assembly procedure is, then carried out to couple between $[K_P]_{Nsc \times Nsc}$ and $[K_{Soil}]_{Nsc \times Nsc}$ to give the overall stiffness matrix $[K_{Overall}]_{Nsc \times Nsc}$ of the plate over on elastic foundation.

It has to be noted that similar condensation procedure should be carried out over the plate load vector, to end up with $\{P\}_{Nsc \times 1}$. The

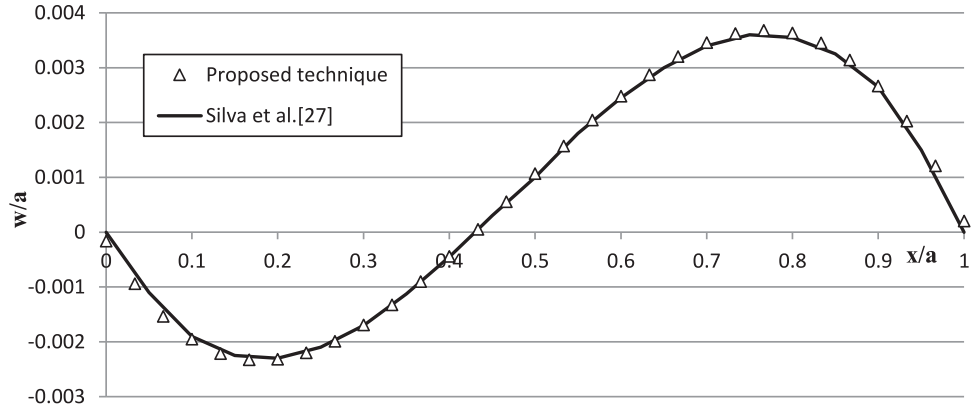

Fig. 6. Deflection along the beam centerline in example 1.

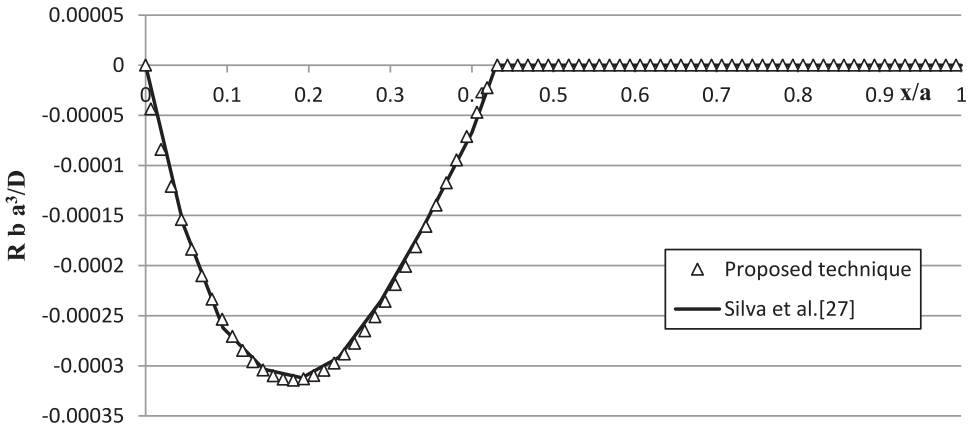

Fig. 7. Contact reaction along the beam centerline in example 1.

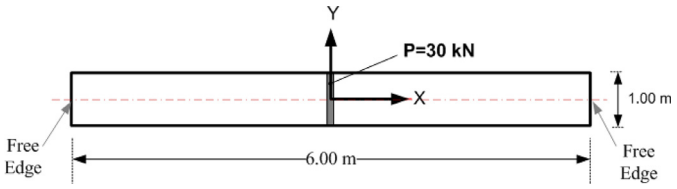

Fig. 8. The free edge beam in example 2.

overall equilibrium equation could be written as follows:

$$\left[K_{Overall}\right]_{Nsc\times Nsc} \times \left\{u_{plate}\right\}_{Nsc\times 1} = \{P\}_{Nsc\times 1} \quad (8)$$

This equation could be solved to compute the plate and foundation deflections in the linear elastic and full contact conditions.

3. The proposed tensionless formulation

In this section, simulation of the foundation as tensionless material is established using the iterative procedures "category 1″ (recall the introduction Section 1). The system of equations in Eq. (8) is then solved; the interaction forces are computed as follows:

$$\left\{F_{Soil\,int.}\right\}_{Nsc\times 1} = \left[K_{Soil}\right]_{Nsc\times Nsc} \times \left\{u_{plate}\right\}_{Nsc\times 1} \quad (9)$$

The most stressed cell is then located and a new static condensation procedure is carried out to eliminate the corresponding DOF from foundation stiffness matrix. This is done to simulate the loss of contact between the plate and the foundation. The overall stiffness matrix is reassembled using the new condensed foundation stiffness matrix. Then the system of equations is resolved. This iterative procedure is repeated until no tensile stress appears. The solution is implemented into a computer code. Fig. 4 demonstrates flowchart of the programmed technique.

It has to be noted that, as an advantage of the present formulation, the iterations are carried out using the system of equations in (8) with dimensions $N_{sc}\times N_{sc}$ instead of solving the overall plate system of equations with dimensions $(3N+N_{sc})\times(3N+N_{sc})$.

4. Extension for elastic-plastic foundation

The previous formulation demonstrated modeling plates on tensionless foundations. The purpose of this section is to extend the use of the proposed formulation in solving plates on elastic-plastic foundations. In such cases, the load is applied in incremental manner. The following few modifications are carried out:

(1) The flow chart given in Fig. 4 is reconsidered for each load increment.

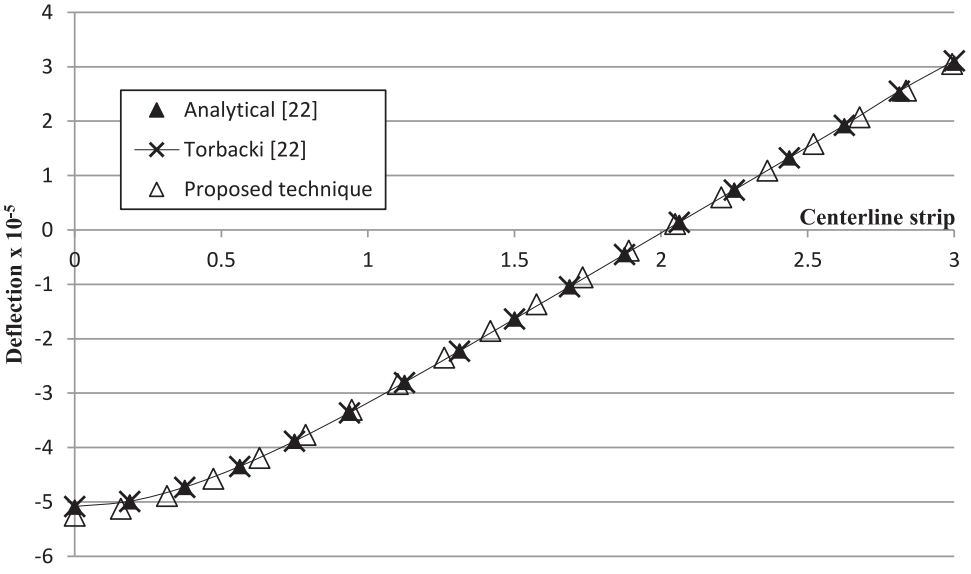

Fig. 9. Deflection along the x-axis in the beam of example 2.

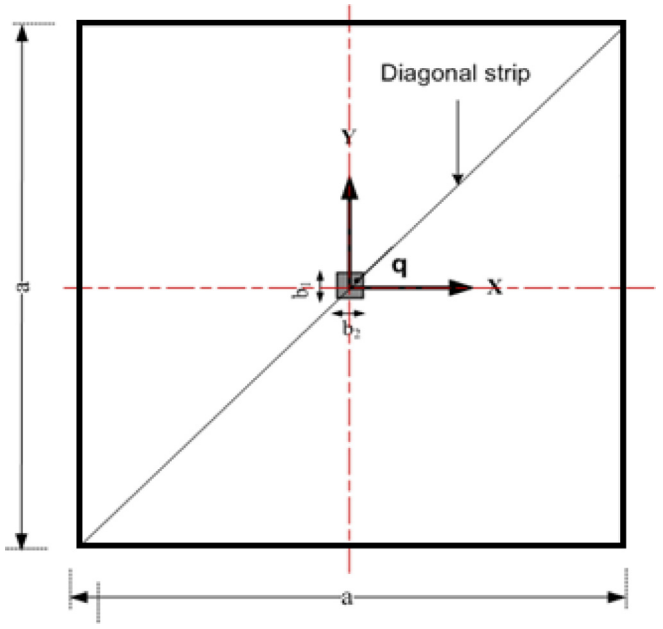

Fig. 10. Free edge square plate in examples 3 and 5.

(2) The deflection of each load increment is added to previous load increment. This forms cumulative deflection results, which are used in computing interaction forces.
(3) A virtual load is applied at failed cells (cells which violated the elastic threshold value). The value of this load is equal to the allowable compressive stress.

Considering these few modifications, the same algorithm presented in Fig. 4 could be reconsidered in straight forward manner.

5. Post-processing of results

After computing the contact zone, internal generalized displacements and stress resultants are determined. First the foundation reactions F(y) are obtained from Eq. (9), hence Eq. (3) is re-used to compute internal generalized displacements.

Stress resultants, moments ($M_{\alpha\beta}$) and shear ($Q_{3\beta}$), could be obtained from the following integral equation:

$$M_{\alpha\beta}(\xi) = \int_{\Gamma(x)} U_{\alpha\beta k}(\xi, x)\, t_k(x) d\Gamma(x) - \int_{\Gamma(x)} T_{\alpha\beta k}(\xi, x)\, u_k(x) d\Gamma(x) + \int_{\Gamma(x)} \left[W_{\alpha\beta}(\xi, x) + \frac{\nu}{(1-\nu)\lambda^2}\delta_{\alpha\beta} \right] q_3(x) d\Gamma(x) + \sum_{N_q} \int_{\Omega(L)} \left[U_{\alpha\beta k}(\xi, y) - \frac{\nu}{(1-\nu)\lambda^2} U_{\alpha\beta\gamma,\gamma}(\xi, y)\delta_{3k} \right] P_k(L) d\Omega(L) + \sum_{N_{sc}} \int_{\Omega(y)} \left[U_{\alpha\beta m}(\xi, y) - \frac{\nu}{(1-\nu)\lambda^2} U_{\alpha\beta\gamma,\gamma}(\xi, y)\delta_{3m} \right] F_m(y)\, d\Omega(y) \quad (10)$$

and

$$Q_{\alpha\beta}(\xi) = \int_{\Gamma(x)} U_{3\beta k}(\xi, x)\, t_k(x) d\Gamma(x) - \int_{\Gamma(x)} T_{3\beta k}(\xi, x)\, u_k(x) d\Gamma(x) + \int_{\Gamma(x)} W_{3\beta}(\xi, x) q_3(x) d\Gamma(x) + \sum_{N_q} \int_{\Omega(L)} \left[U_{3\beta k}(\xi, y) - \frac{\nu}{(1-\nu)\lambda^2} U_{3\beta\gamma,\gamma}(\xi, y)\delta_{3k} \right] P_k(L) d\Omega(L) + \sum_{N_{sc}} \int_{\Omega(y)} \left[U_{3\beta m}(\xi, y) - \frac{\nu}{(1-\nu)\lambda^2} U_{3\beta\gamma,\gamma}(\xi, y)\delta_{3m} \right] F_m(y)\, d\Omega(y) \quad (11)$$

where the kernels $U_{\alpha\beta k}$,$T_{\alpha\beta k}$ are their relevant derivatives could be obtained from reference [11]. Relevant values of boundary tractions, generalized displacements ({t} and {u}) could be generated from the matrix [PBIV] in Eq. (6).

6. Numerical examples

In this section, several examples are solved and results are compared to analytical and previously published results to verify the proposed formulation.

6.1. Example 1: simply supported beam on tensionless winkler foundation

The simply supported beam in Fig. 5 is considered in this example. The beam is modeled as thick plate with dimensions a = 10, b = 1.0 and

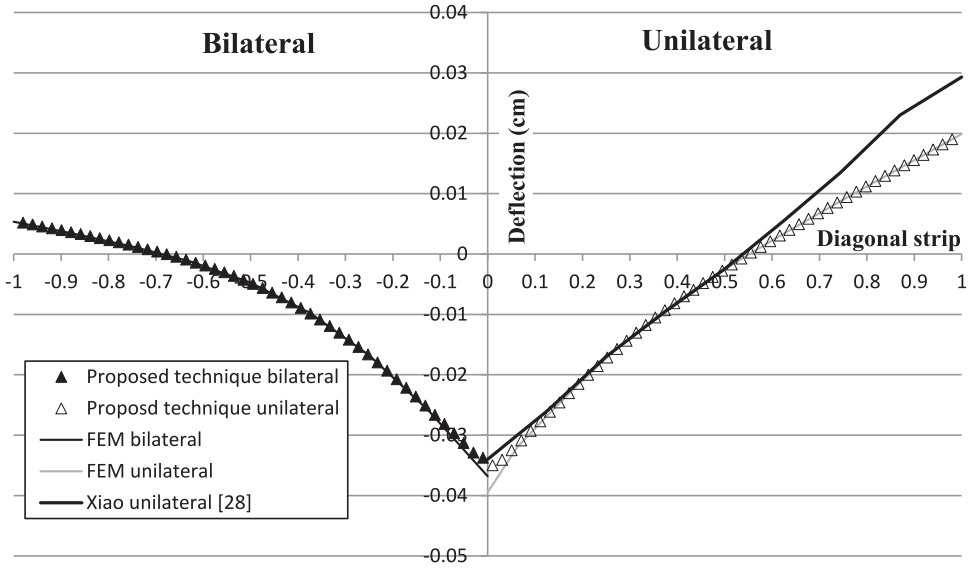

Fig. 11. Deflections along the diagonal strip for plate thickness = 30 cm in example 3.

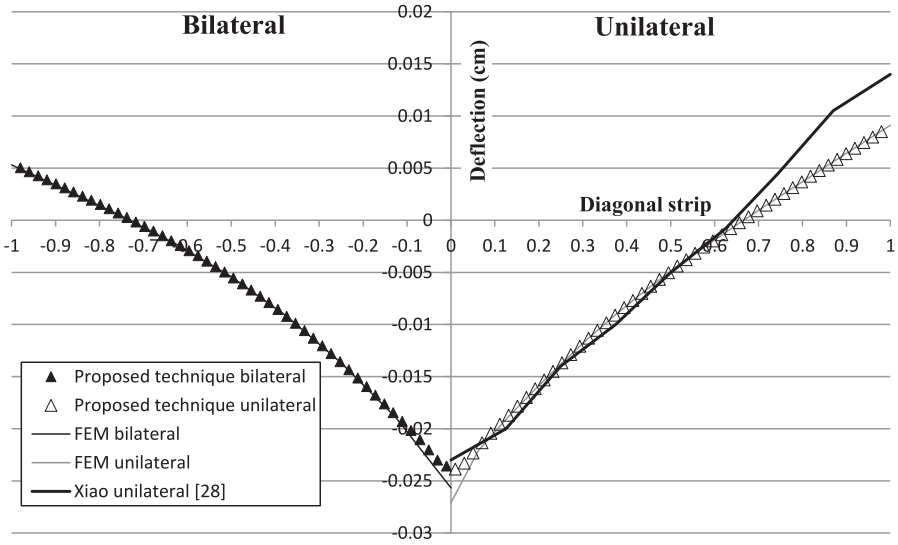

Fig. 12. Deflections along the diagonal strip for plate thickness = 40 cm in example 3.

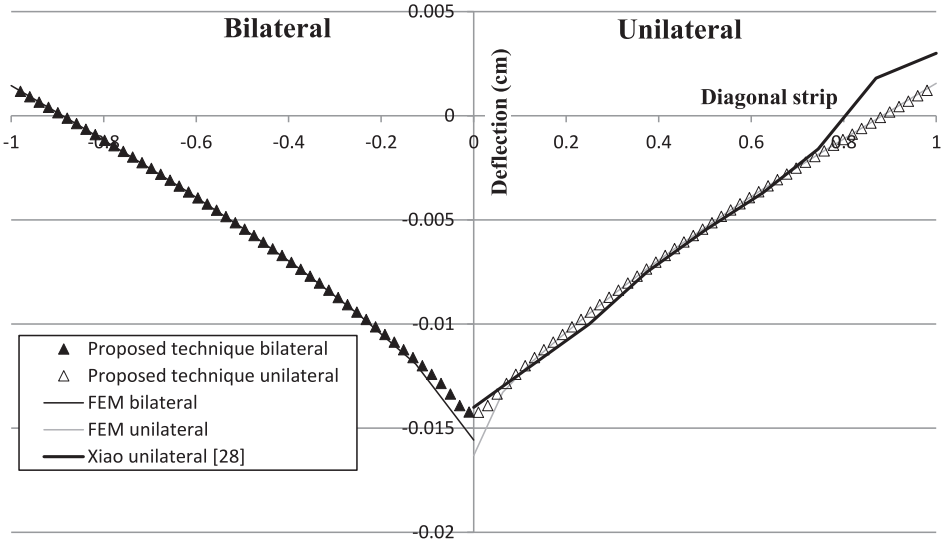

Fig. 13. Deflections along the diagonal strip for plate thickness = 60 cm in example 3.

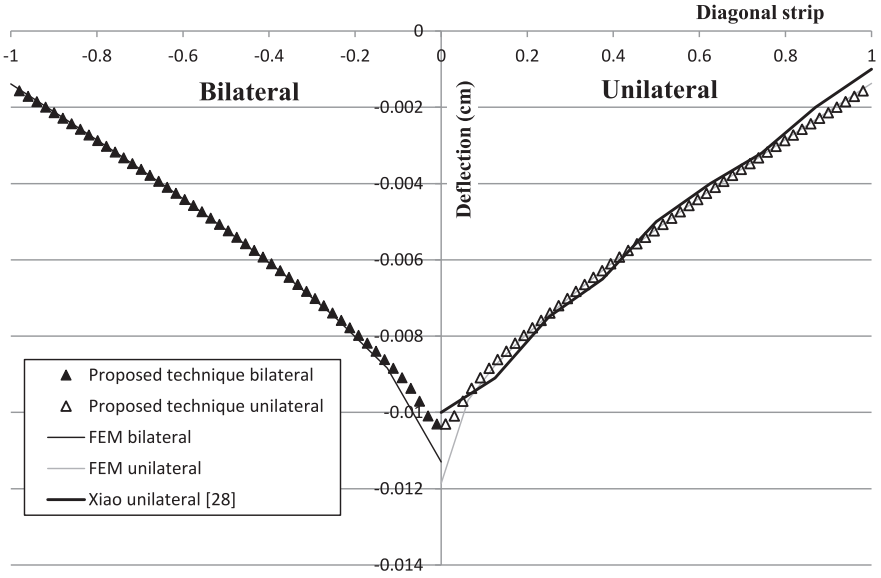

Fig. 14. Deflections along the diagonal strip for plate thickness = 80 cm in example 3.

Table 1
Contact region pattern; deflection and bending moment contour maps for thickness = 30 cm in example 3.

Item	Proposed technique results	FEM results
Contact region	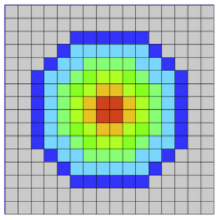	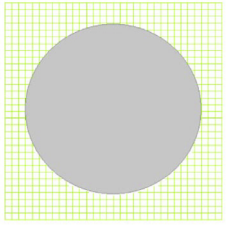
unilateral deflections	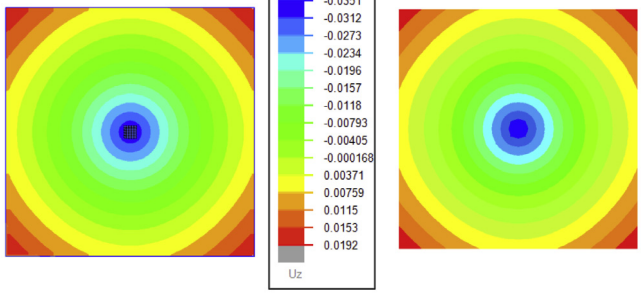	
unilateral bending moments	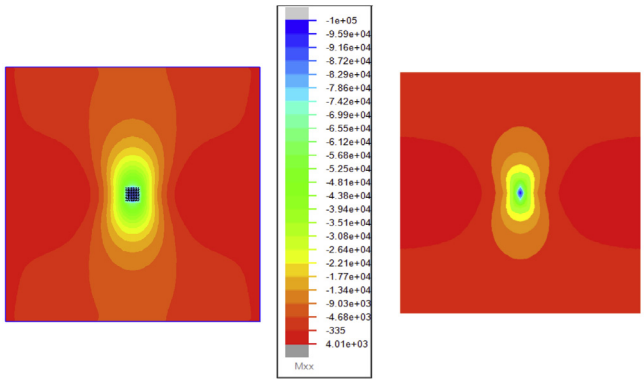	

Table 2
Deflections and bending moments at center of the plate in example 3.

t/a	Plate model	Result of	Bilateral foundation		Unilateral foundation	
			W_{max} (cm)	M_{max} ($\times 10^5$ N cm)	W_{max} (cm)	M_{max} ($\times 10^5$ N cm)
0.075	Kirchhoff	Xiao [28]	0.029947	0.76436	0.031942	0.77746
		Analytical [31]	0.029597	0.76121	0.031344	0.7743
	Reissner	Xiao [28]	0.033593	0.9178	0.03571	0.9318
		Analytical [32]	0.033335	0.91217	0.035083	0.92548
		Proposed technique 16 × 16	0.033758	0.97026	0.035082	0.98908
		FEM 16 × 16	0.03681	0.973095	0.03806	0.991336
		FEM 32 × 32	0.03823	1.245049	0.039475	1.263609
		FEM 64 × 64	0.03971	1.503709	0.04095	1.52238
		FEM 128 × 128	0.04124	1.758721	0.04248	1.777329
0.10	Kirchhoff	Xiao [28]	0.020562	0.85509	0.021287	0.86783
		Analytical [31]	0.020206	0.85184	0.020564	0.86407
	Reissner	Xiao [28]	0.023548	1.13123	0.024273	1.14375
		Analytical [32]	0.023296	1.12539	0.023634	1.13757
		Proposed technique 16 × 16	0.023576	1.1825	0.023951	1.1935
		FEM 16 × 16	0.02567	1.071322	0.02601	1.083058
		FEM 32 × 32	0.02677	1.337081	0.0271	1.348448
		FEM 64 × 64	0.02791	1.594	0.02822	1.604972
		FEM 128 × 128	0.02907	1.848564	0.02937	1.859178

(*continued on next page*)

Table 2 (*continued*)

t/a	Plate model	Result of	Bilateral foundation		Unilateral foundation	
			W_{max} (cm)	M_{max} ($\times 10^5$ N cm)	W_{max} (cm)	M_{max} ($\times 10^5$ N cm)
0.15	Kirchhoff	Xiao [28]	0.011997	0.97961	0.012377	0.98032
		Analytical [31]	0.011747	0.97745	0.011749	0.97809
	Reissner	Xiao [28]	0.014365	1.6114	0.014393	1.6121
		Analytical [32]	0.014066	1.60388	0.014069	1.6045
		Proposed technique 16×16	0.01427	1.6580	0.014271	1.6585
		FEM 16×16	0.01557	1.202636	0.01557	1.20333
		FEM 32×32	0.01631	1.463089	0.01632	1.46371
		FEM 64×64	0.01708	1.718589	0.01708	1.7191804
		FEM 128×128	0.01785	1.97278	0.01786	1.973364
0.20	Kirchhoff	Xiao [28]	0.008621	1.04231	0.008622	1.04233
		Analytical [31]	0.008339	1.04001	0.008339	1.04001
	Reissner	Xiao [28]	0.010445	2.17191	0.010473	2.17193
		Analytical [32]	0.010191	2.16231	0.010191	2.16231
		Proposed technique 16×16	0.010336	2.2132	0.010336	2.2132
		FEM 16×16	0.0113	1.268764	0.01130	1.268764
		FEM 32×32	0.01186	1.526816	0.01186	1.526816
		FEM 64×64	0.01244	1.781687	0.01244	1.781687
		FEM 128×128	0.01302	2.035717	0.01302	2.035717
0.25	Kirchhoff	Xiao [28]	0.007064	1.07235	0.007064	1.07235
		Analytical [31]	0.006829	1.06945	0.006829	1.06945
	Reissner	Xiao [28]	0.008615	2.8399	0.008615	2.8399
		Analytical [32]	0.008358	2.82981	0.008358	2.82981
		Proposed technique 16×16	0.008452	2.8771	0.008452	2.8771
		FEM 16×16	0.00923	1.30101	0.00923	1.30101
		FEM 32×32	0.00969	1.55782	0.00969	1.55782
		FEM 64×64	0.01015	1.81236	0.01015	1.81236
		FEM 128×128	0.01062	2.06631	0.01062	2.06631

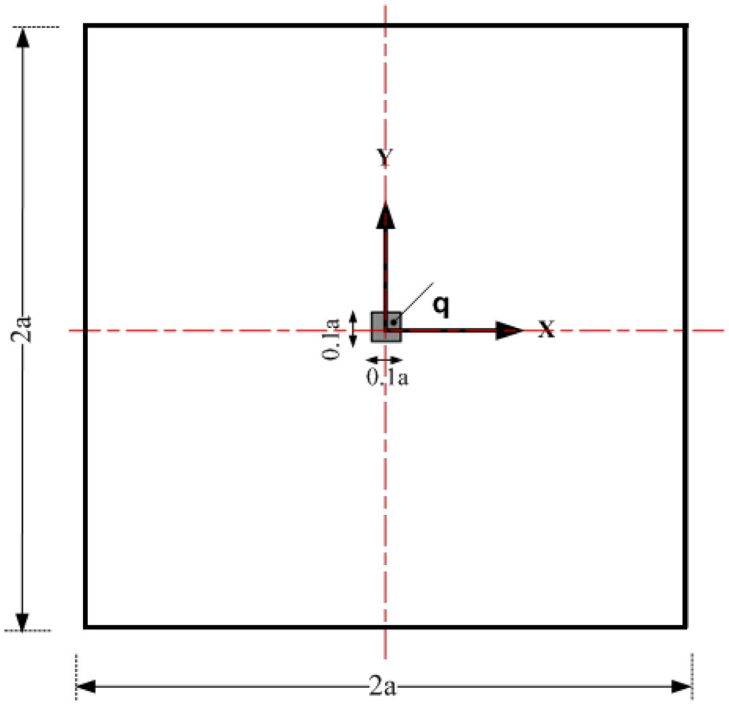

Fig. 15. Free edge square plate in example 4.

t = 0.4, the Young's modulus is E = 10^6, Poisson's ratio of the plate material is $\nu = 0$. Concentrated moments M = 100 is applied as shown in Fig. 5. The foundation is modeled as Winkler foundation with 40 cells with stiffness parameter K = 71.68. It has to be noted that any unit system is applicable. The boundary is divided into 10×1 boundary elements. In Ref. [27], Silva et al. considered the same problem using 20 isoparametric finite elements with eight nodes.

The beam is solved using the proposed technique and results are compared to results obtained from Silva et al. [27]. It can be seen from the results (see Figs. 6 and 7) that the proposed technique obtained the same contact length (x/a = 0.43) as that in Ref. [27]. In addition, deflection along centerline of the beam (x-axis) and contact reaction are in a good agreement with results in Ref. [27]. It has to be noted that in Fig. 7, D is the plate rigidity and the R is contact reaction.

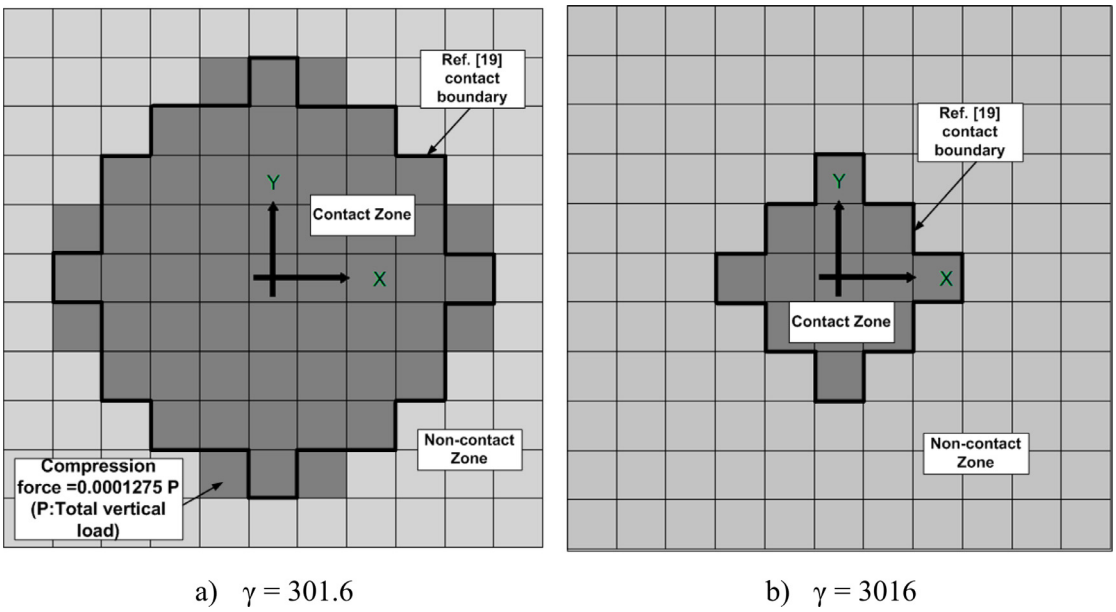

Fig. 16. Contact zones for different relative stiffness parameters γ in example 4.

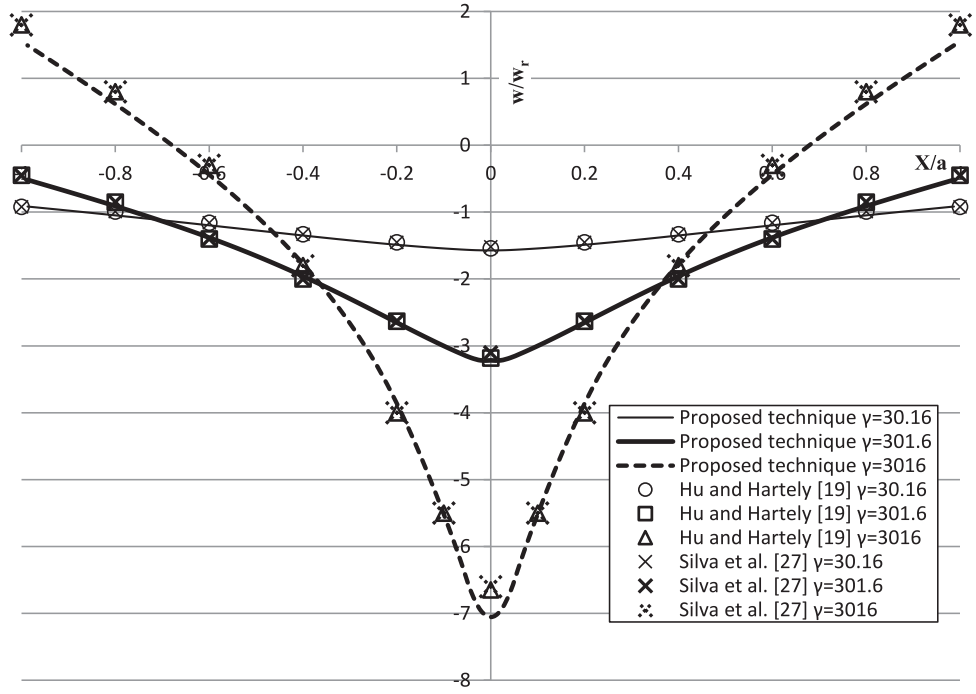

Fig. 17. Deflections along the centerline strip in example 4.

6.2. Example 2: free edges beam on tensionless Winkler foundation

The free edge beam (previously considered in Ref. [22]) shown in Fig. 8 is considered in this example. The beam is loaded by concentrated load of 30 kN at its center and has dimensions of L = 6 m, b = 1.0 m and t = 0.47 m. The used Young's modulus is $E = 2\times10^7$ kN/m^2, Poisson's ratio is $\nu = 0$. The beam is modeled as thick plate with 10×1 boundary elements, and foundation is modeled as Winkler foundation with 60 cells having stiffness parameter $K = 250{,}000$ kN/m^3. The load is applied using small cell (0.1 m × 1 m) in this work. In Ref. [22], Torbacki modeled the beam as beam element according to Euler–Bernoulli and foundation using special finite elements of zero thickness designated for foundation modeling.

Based on symmetry condition, only one half of the beam is considered. The analytical contact length is 4.034 m as given in Ref. [22].The contact length of the proposed formulation is 4.00 m, due to discritization. Fig. 9 demonstrates analytical results [22], results of Torbacki [22] and the proposed technique deflections along the beam centerline. It can be seen that results are in good agreement.

6.3. Example 3: free edge square plate on tensionless Winkler foundation

In this example, the free edge square plate (previously considered in Ref. [28]) shown in Fig. 10 is considered. The foundation is discretized into 16×16 Winkler cells. The plate side length is a = 400 cm. The used Young's modulus is $E = 2.6\times10^6$ N/cm^2, Poisson's ratio is $\nu = 0.15$.

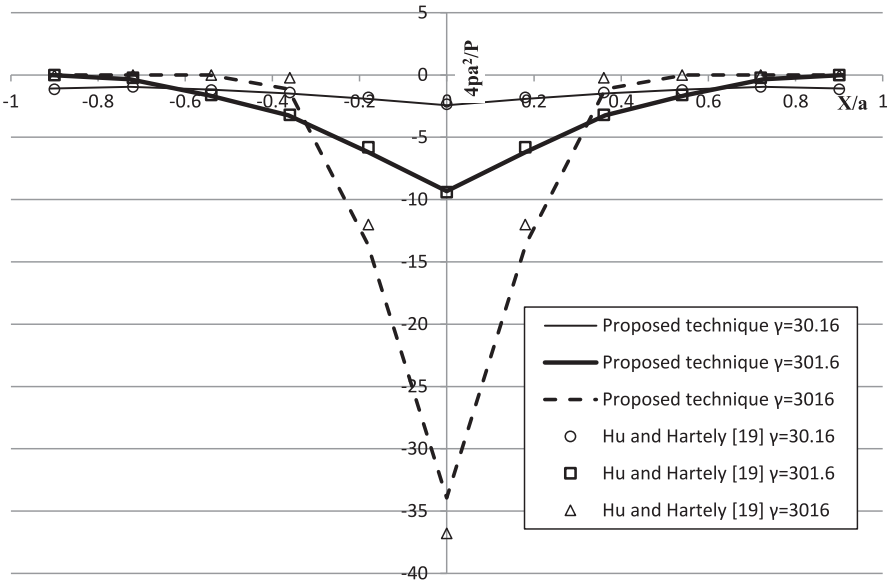

Fig. 18. Contact pressure along the centerline strip in example 4.

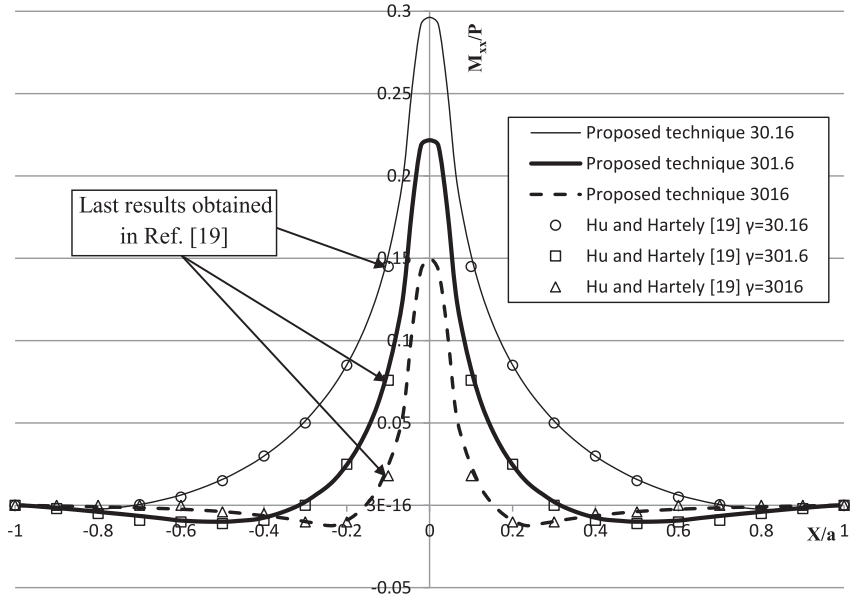

Fig. 19. Bending moments M_{xx} along the centerline strip in example 4.

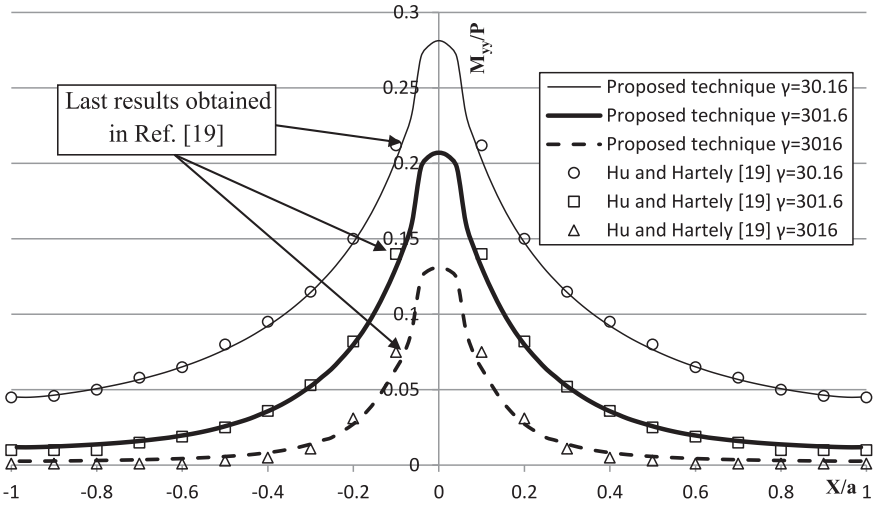

Fig. 20. Bending moments M_{yy} along the centerline strip in example 4.

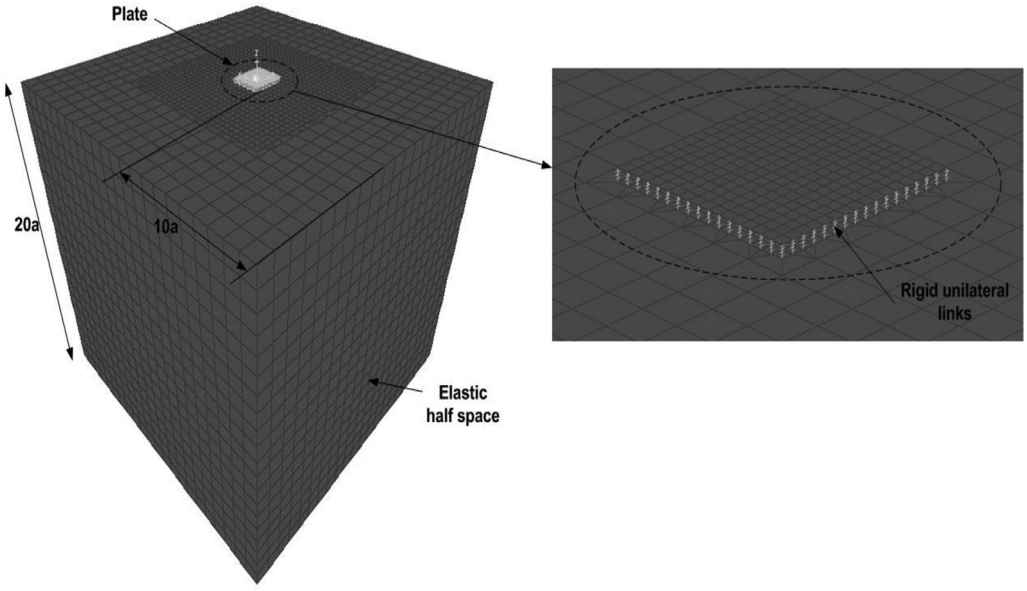

Fig. 21. Finite element model of example 5.

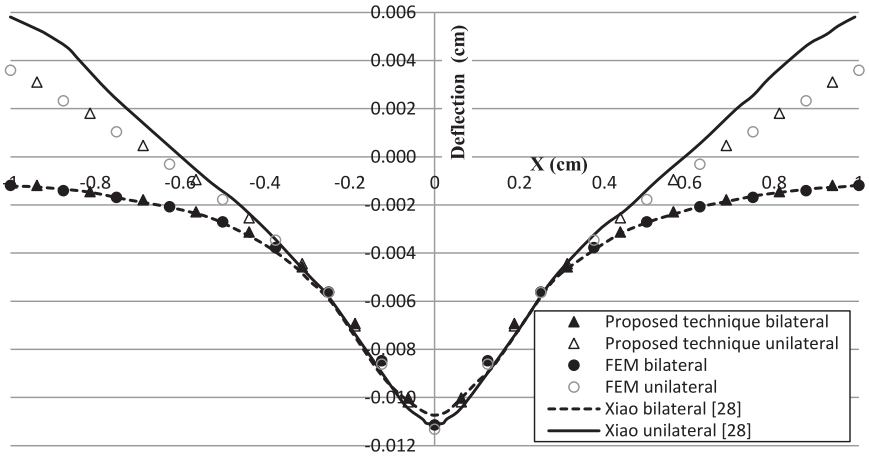

Fig. 22. Deflections along the diagonal strip for plate thickness = 2 cm in example 5.

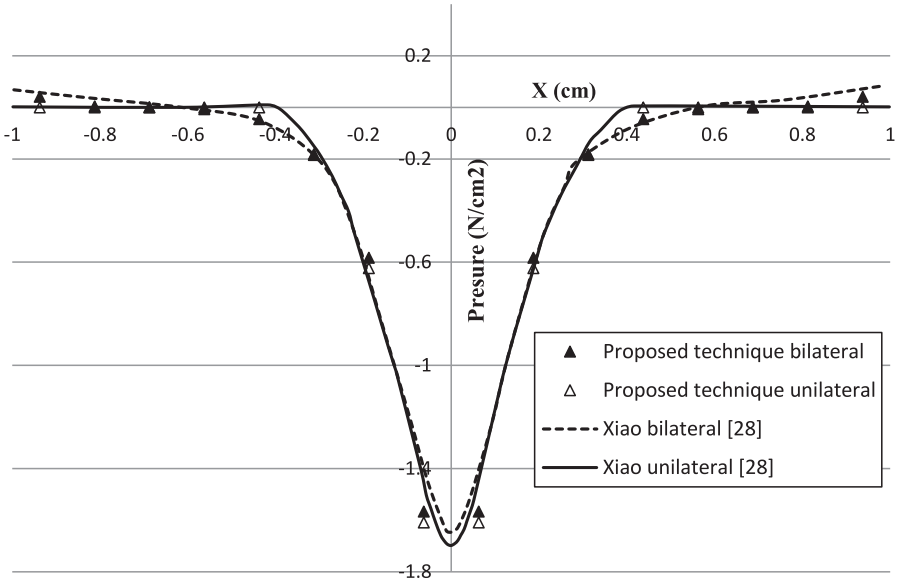

Fig. 23. Contact pressure along the diagonal strip for plate thickness = 2 cm in example 5.

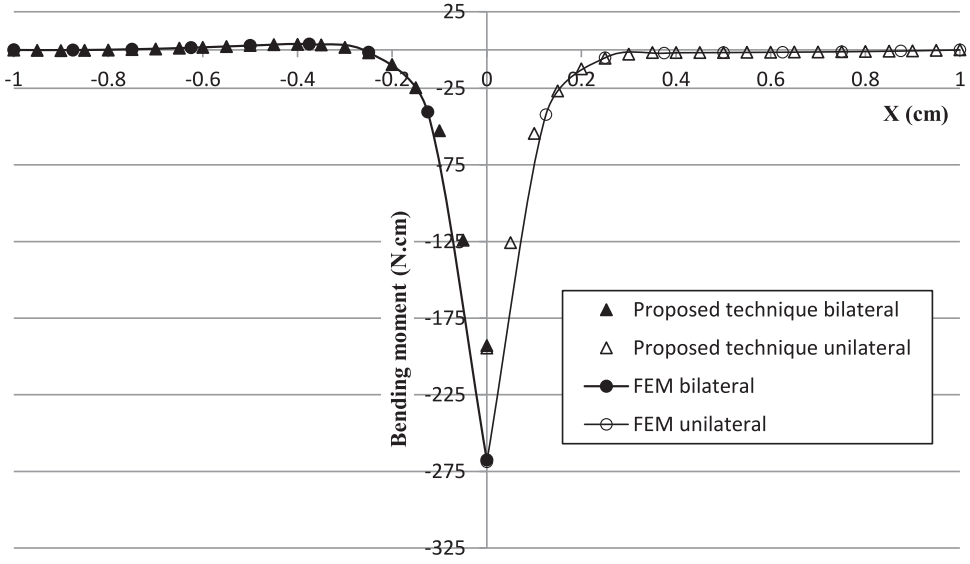

Fig. 24. Bending moments along the diagonal strip for plate thickness = 2 cm in example 5.

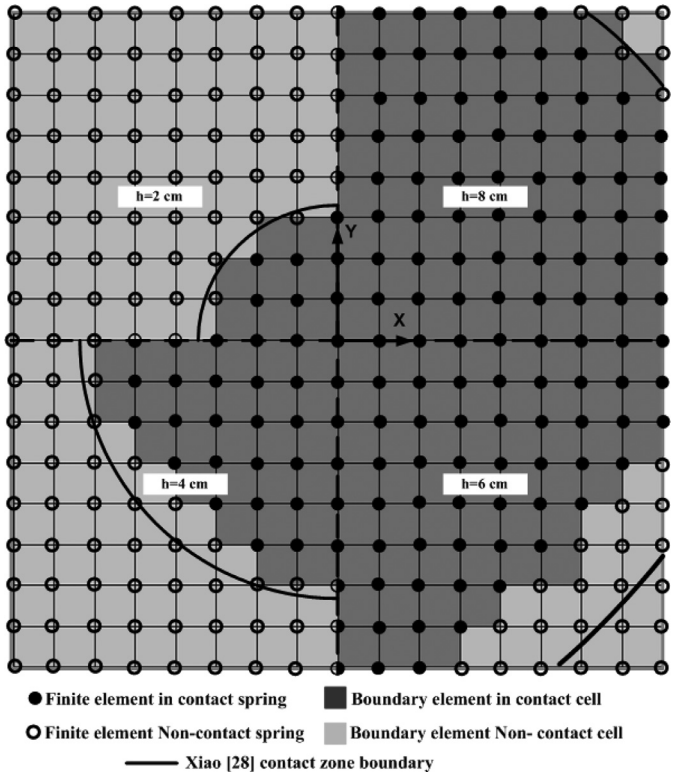

Fig. 25. Contact zones for different plate thicknesses in example 5 (the second analyzed case).

Different plate thicknesses (t) are employed 30, 40, 60, 80, 100 cm to allow comparison with results of Ref. [28]. The foundation stiffness parameter K is 500 N/cm^3. Plate is loaded by patch distributed load q = 1000 N/cm^2 over area of 20 cm × 20 cm at its center. In Ref. [28], Xiao modeled the problem as thick plate using 64 constant boundary elements and the foundation using 16 × 16 domain square cells.

Figs. 11–14 demonstrate the proposed technique deflections along the diagonal strip (indicated in Fig. 10) for different thicknesses of plate, together with Xiao [28] results. It can be seen that results are in a good agreement with Ref. [28] except at the vicinity of corners, which some inaccurate results due to the implemented formulation of Ref. [28]. Therefore in this paper a FEM model is prepared using 32 × 32 thick plate elements and Winkler foundation is modeled via unilateral links. The results of the FEM are plotted also in Figs. 11–14, from these figures, it can be seen that the proposed formulation results near corners are in good agreement with the FEM results. However, FEM presents some overestimated values in the bending moment under load. Table 1 demonstrates the contact region pattern; deflection and bending moment contour maps for plate thickness 30 cm. Table 2 demonstrates deflection and bending moment values at plate center point based on the proposed technique, FEM, Xiao [28] and analytical solutions obtained from Bu and Yan [32]. It can be seen from the results that the present formulation results are in good agreement with the analytical values with coarse discretization (16 × 16 for foundation cells). However, in the FEM case, results in the vicinity of stress concentration (under load) are mesh dependent with some overestimated peaks in bending moment. This demonstrates the stability of the proposed formulation results.

6.4. Example 4: free edge square plate on tensionless half space foundation

In this example, the free edge square thin plate (previously considered in Refs. [19,27]) shown in Fig. 15 is considered with $\nu = \nu_s = 0.15$. The plate is loaded by concentrated load P at its center. Hu and Hartely [19] modeled each side of the plate using one fifth-order boundary element and half space is discretized into 11 × 11 constant contact elements. In [19], results are given for several values of γ (foundation/plate relative stiffness parameter), which is defined as follows:

$$\gamma = \frac{\pi E_s a^3}{D(1-\upsilon_s^2)} \tag{12}$$

where, D is the plate rigidity and E_s, ν_s are foundation Young's modulus and Poisson's ratio respectively. Silva et al. [27] modeled the plate using 36 finite elements. In this paper, the plate three values of relative stiffness parameter are considered $\gamma = 30.16, 301.6, 3016$ to allow comparison with results of Ref. [19,27]. The foundation is discretized into 11 × 11 cells.

Fig. 16 demonstrates the contact zones of proposed technique and results of Hu and Hartely [19]. It can be seen that the present formulation contact zone is in good agreement with that obtained from Ref. [19]. Figs. 17 and 18 demonstrate the deflection and contact pressure along centerline strip of the plate respectively in which the associated displacement parameter given by these authors [19] for a rigid square plate is:

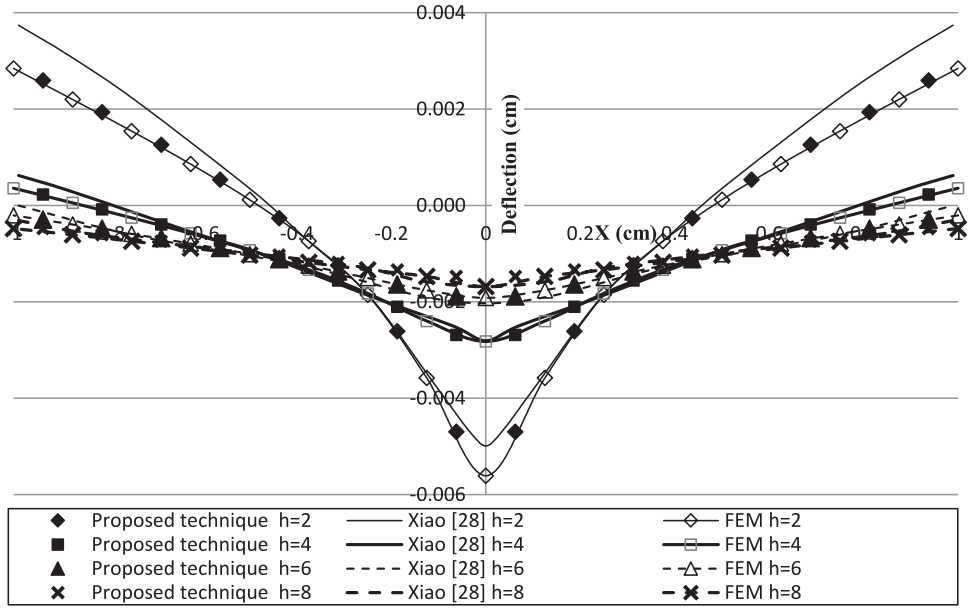

Fig. 26. Deflections along the diagonal strip for plate different thicknesses in example 5 (the second analyzed case).

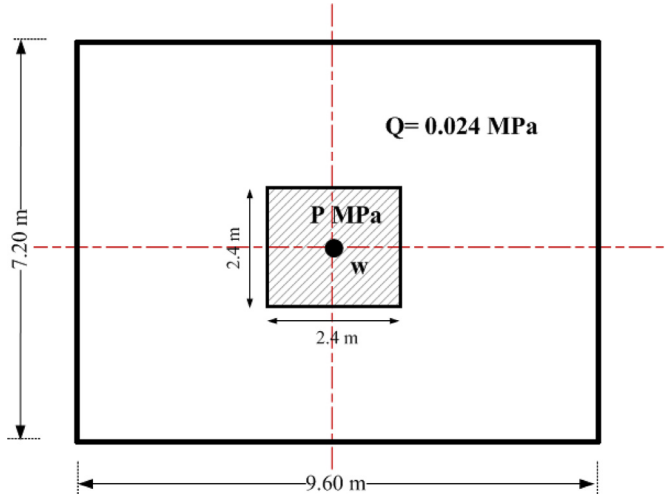

Fig. 27. The plate on elastic-plastic Winkler foundation in example 6.

$$w_r = \frac{0.913\left(1-\upsilon_s^2\right)P}{2aE_s} \tag{13}$$

where, P is the total vertical load on the plate.

Figs. 19 and 20 demonstrate bending moments M_{xx}, M_{yy} along centerline strip of the plate respectively. It has to be noted that, bending moment results could not be computed in the formulation of Hu and Hartely [19] under load. Moreover, it is not given in Silva et al. [27].

Generally, it can be seen that the present formulation results are in good agreement with those of Hu and Hartely [19] and Silva et al. [27].

6.5. Example 5: free edge square plate on tensionless half space foundation

In this example, the free edge square plate resting on elastic half space (previously considered in Ref. [28]) shown in Fig. 10 is considered. The foundation is discretized into 16×16 cells. The plate side length is $a=100$ cm and thickness is 2 cm. The used Young's modulus is $E=2.0\times10^6$ N/cm^2, Poisson's ratio is $\nu=0.3$. Foundation modulus is $E_s=3000$ N/cm^2, Poisson's ratio is $\nu_s=0.4$. The plate is loaded by a concentrated load $P=1000$ N. Xiao [28] modeled the problem as thick plate using 64 constant boundary elements on the boundary and the foundation using 16×16 domain square cells.

Results of the present formulation are compared to those obtained from Xiao [28]. Similar to example 3, a FEM model is considered, in which the plate is modeled as 16×16 thick plate elements and half space is modeled using 3D solid elements extended to ten times as the plate width a from each side. Plate elements are connected to solid elements via unilateral rigid links. This model is shown in Fig. 21.

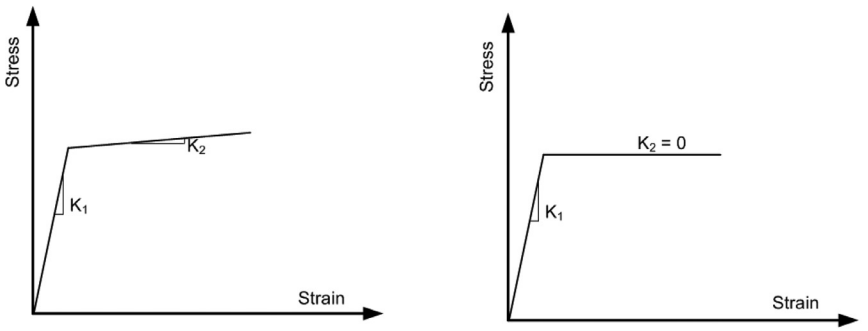

a) Foundation behavior in Ref. [33]. b) The considered foundation behavior.

Fig. 28. Foundation behavior in example 6. (a) Foundation behavior in Ref. [33]. b) The considered foundation behavior.

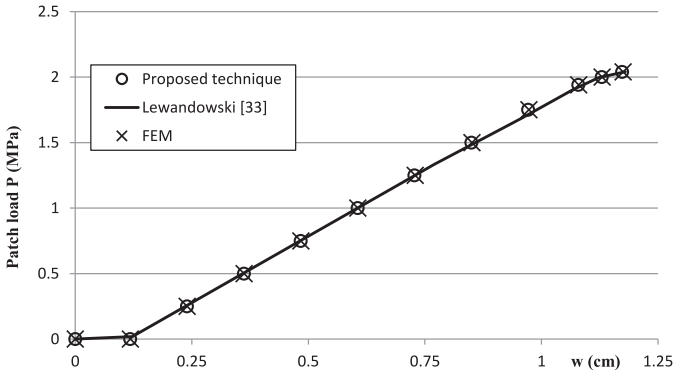

Fig. 29. The center point deflection verses the patch load P in example 6.

Figs. 22 and 23 demonstrate the proposed technique deflections and foundation reactions along the diagonal strip (indicated in Fig. 10), together with results of Xiao [28] and FEM results. It can be seen that unlike the results of Ref. [28], the present formulation results are accurate in the vicinity of corners. Fig. 24 demonstrates a comparison of bending moments along the same strip. It can be seen that results are in good agreement except for some over estimated peaking values under stress concentration zones in bending moments in FEM results.

The plate in Ref. [28] is analyzed another time with different plate thicknesses (t) 2, 4, 6, 8, 10 cm. In this case another foundation modulus $E_s = 8600\ N/cm^2$ is used.

Fig. 25 demonstrates the contact zones to the proposed technique, Xiao and FEM. Despite the simplicity of the present formulation compared with the FEM models, it can be seen that the contact zone of the present formulation agrees with that of the FEM; whereas, results of Ref. [28] are slightly different especially for h = 6 cm.

Fig. 26 demonstrates a comparison of deflection along the same diagonal strip for different plate thicknesses together with results of Xiao [28].

6.6. Example 6: free edge plate on elastic-plastic Winkler foundation

The plate shown in Fig. 27 is considered in this example. The used Young's modulus is 23 GPa, Poisson's ratio is $\nu = 0.17$, soil Winkler modulus is K = 20 MPa and the allowable compressive stress of soil is q = 0.2 MPa. The plate has dimensions a = 9.6 m, b = 7.2 m and t = 1.2 m. The whole plate domain is uniformly loaded by Q = 0.024 MPa together with incrementally increasing load patch P (in MPa) over the hatched area.

It has to be noted that the previously published results of this example in Ref. [33] are based on assuming that the foundation behaves as bilinear curve as shown in Fig. 28 with initial modulus $K_1 = 20$ MPa and $K_2 = 0.1$ MPa. In this paper the foundation behavior is assumed as elastic perfectly plastic i.e. $K_1 = 20$ MPa and $K_2 = 0$. For the purpose of verification, additional FEM model is prepared, in which the plate is modeled as 32×24 plate elements and Winkler foundation is modeled via unilateral links with $K_1 = 20$ MPa and $K_2 = 0$.

Fig. 29 demonstrates the relationship between the applied load patch P with the deflection at plate center w. It can be seen that results are in a good agreement with those obtained by Lewandowski [33] and FEM results. Fig. 30 demonstrates the boundary of the plastic zone for two different load levels, which demonstrated the excellent agreement.

6.7. Example 7: free edge plate on elastic-plastic and tensionless Winkler foundation

The purpose of this example is to demonstrate the use of the proposed formulation in solving plates on both elastic-plastic and tensionless foundation. The plate shown in Fig. 31 is considered in this example with dimensions a = 4.8 m, b = 3.6 m and t = 0.4 m. All properties are taken the

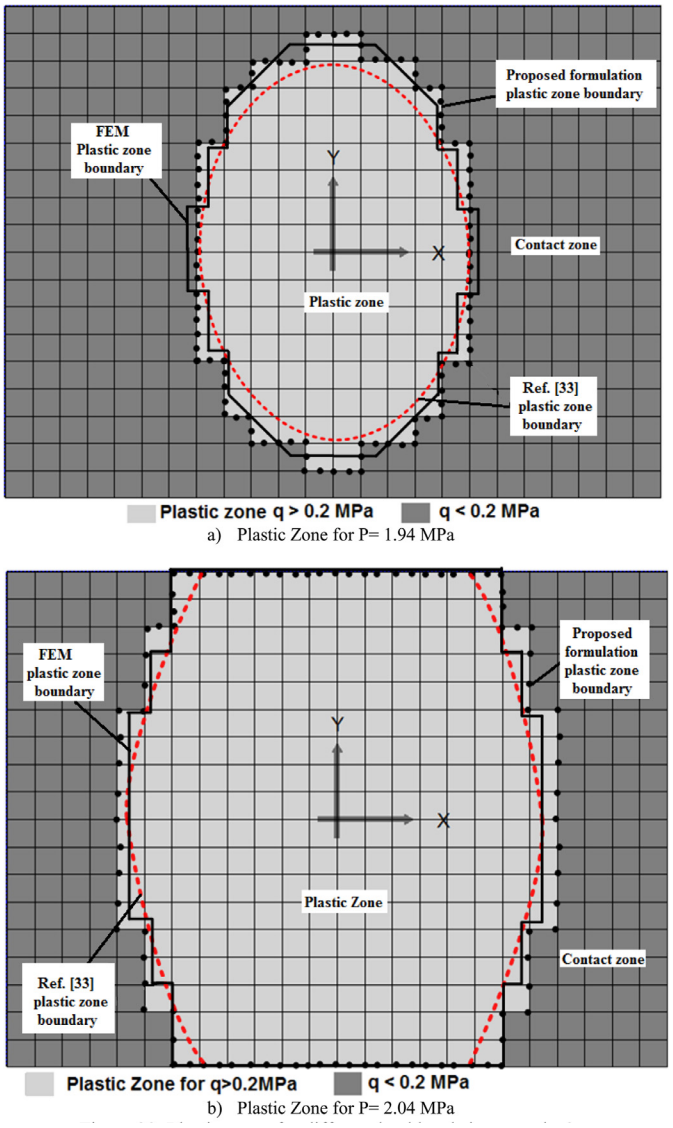

Fig. 30. Plastic zones for different load levels in example 6.

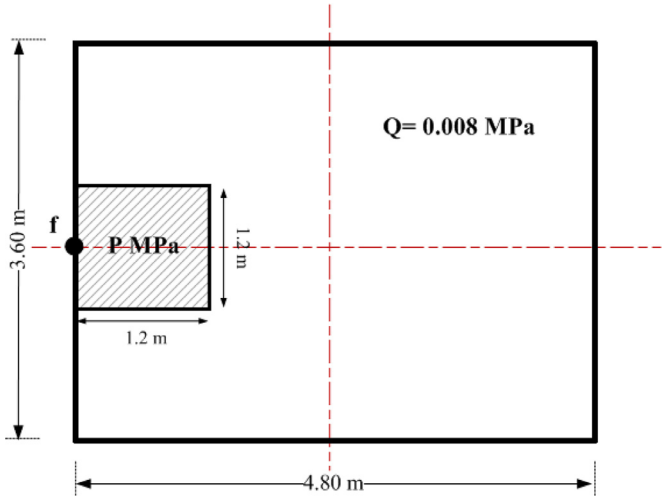

Fig. 31. The plate on elastic-plastic and tensionless Winkler foundation in example 7.

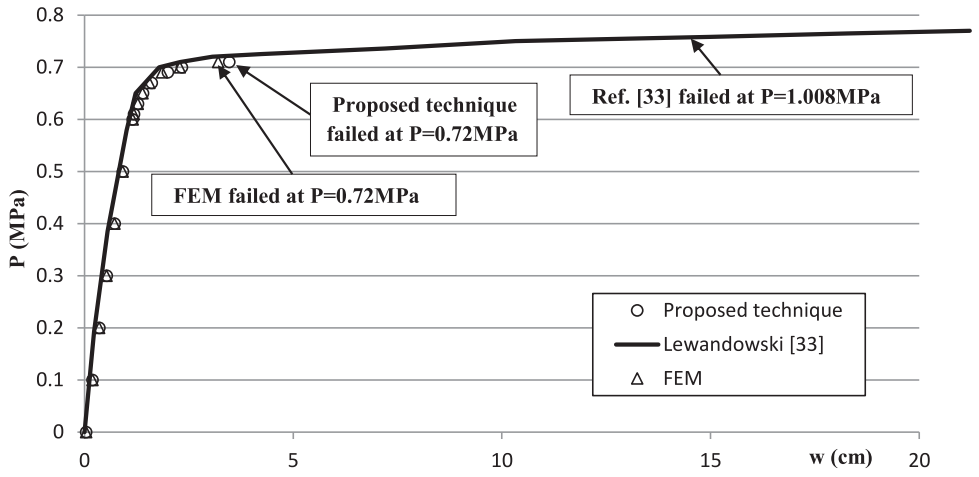

Fig. 32. Deflections at point f for different load level in example 7.

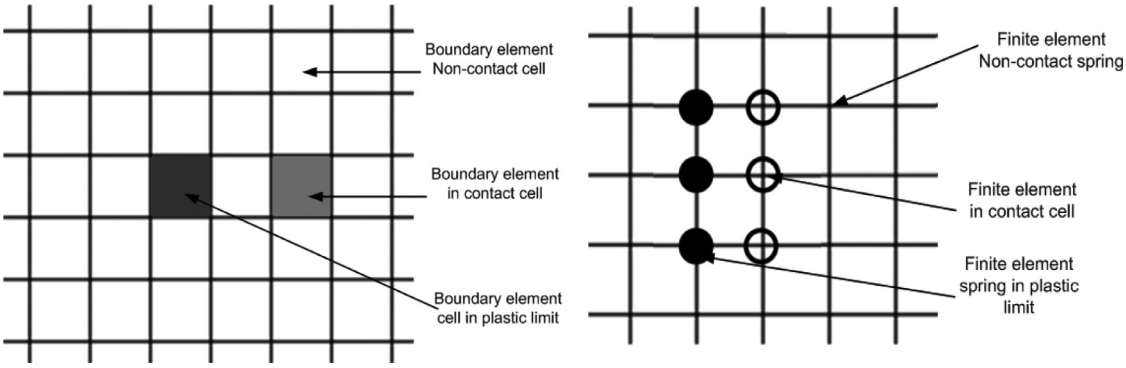

Fig. 33. The notations used in example 7.

same as those presented in example 6. The whole plate domain is uniformly loaded by Q = 0.008 MPa together with incrementally increasing load patch P (in MPa) over the hatched area. This example is previously considered in Ref. [33] with bilinear foundation behavior ($K_1 = 20$ MPa and $K_2 = 0.1$ MPa). In this paper the foundation behavior is assumed elastic perfectly plastic i.e. $K_1 = 20$ MPa and $K_2 = 0$. Similar to example 6, a FEM model is also prepared to verify the results of this problem. In this model, the plate is modeled as 32×24 plate elements and Winkler foundation is modeled via unilateral links with $K_1 = 20$ MPa and $K_2 = 0$.

Fig. 32 demonstrates the relationship between the applied load patch P with deflection at point f. It can be seen that results are in a good agreement with Lewandowski [33]. At a load level of P = 0.72 MPa, instability in the present formulation and in the FEM results are detected which demonstrate failure. In Ref. [33], on the other hand, the plate can carry a load up to P = 1.008 MPa as $K_2 = 0.1$ MPa. Fig. 33 demonstrates notations used to represent contact and plastic zones demonstrated in Fig. 34.

6.8. Example 8: irregular plate on tensionless Winkler foundation

The purpose of this example is to demonstrate the applicability of the proposed technique in solving irregular shaped plate. Consider the free edged irregular plate resting on tensionless foundation shown in Fig. 35. The Plate is loaded by three column loads with different intensities as shown in Fig. 35. The plate thickness t is 25 cm, the Young's modulus is $E = 2 \times 10^6$ t/m^2 and the Poisson's ratio is $\nu = 0.2$. The foundation is modeled as Winkler foundation. The foundation stiffness parameter K is 1500 t/m^3.

Fig. 36 demonstrates the final contact zone of the proposed technique compared to results obtained from FEM model. Fig. 37 demonstrates the deflection along strip 1. In addition, Fig. 38 demonstrates the bending moments along the same strip.

It can be seen that the results obtained from the proposed technique are in good agreement with FEM results.

7. Conclusions

In this paper, solution of plates on tensionless Winkler or elastic half space foundation is presented using an efficient improved (BEM-based) FEM formulation. The plate stiffness matrix and load vector are extracted using boundary element formulation in innovative manner. The Mindlin equation is used to calculate the elastic half space stiffness matrix. A coupling technique is used to assemble the overall stiffness matrix of the problem to produce a finite element like system of equations. An iterative technique is used to eliminate the tensile stresses. The technique is also extended to plates over elastic-plastic Winkler foundation.

Several examples are presented and from results it can be concluded that the main advantages of this technique are:

1. The simplicity in dealing with the nonlinearity nature of the problem.
2. The stability of results in stresses concentration zones.
3. The accurate results near corners unlike previously published boundary element formulations.
4. The ability of solving any geometry and any boundary conditions.

Extending the present formulation to plates over elastic-plastic half space requires additional modifications which will be considered by the authors in future work. Moreover, the presented procedure will be used in straightforward manner to couple super and sub structures, which also will be considered as future work.

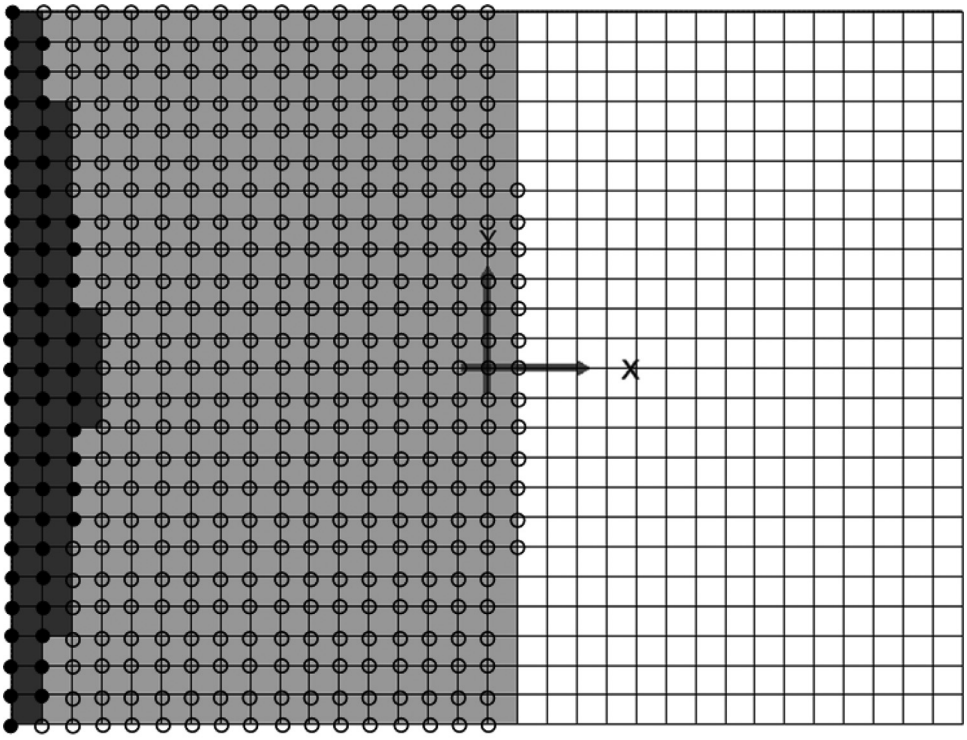

a: Contact and plastic zones for P= 0.6 MPa.

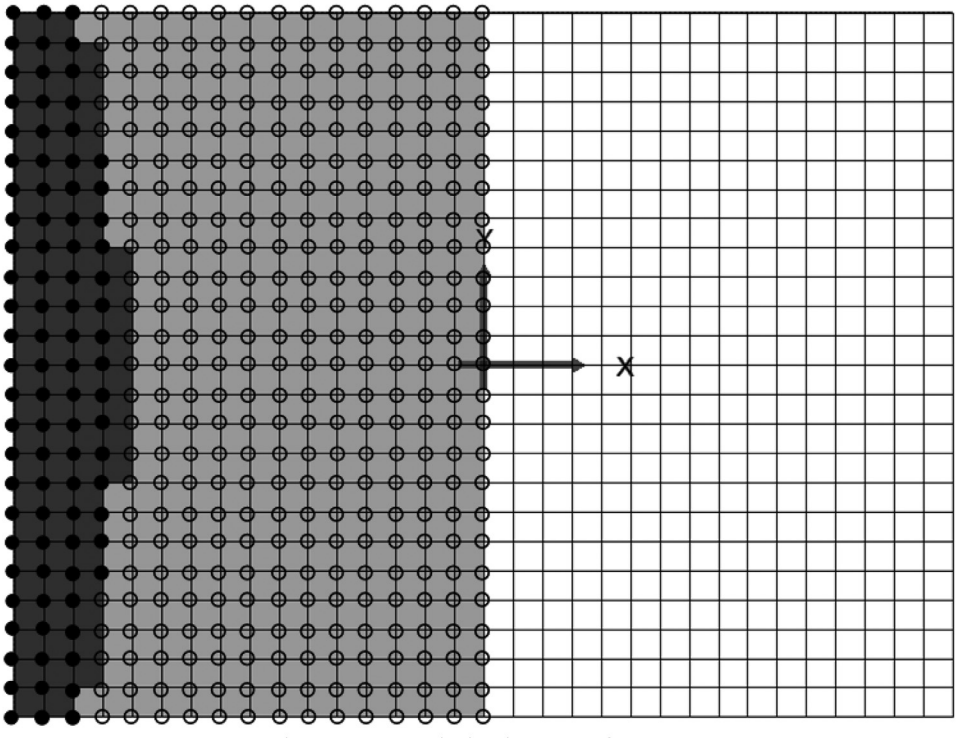

b: Contact and plastic zones for P= 0.63 MPa.

Fig. 34. Contact and plastic zones for different load levels up to failure in example 7. (a) Contact and plastic zones for P = 0.6 MPa. (b) Contact and plastic zones for P = 0.63 MPa. (c) Contact and plastic zones for P = 0.65 MPa. (d) Contact and plastic zones for P = 0.7 MPa. (e) Contact and plastic zones for P = 0.71 MPa. (f) Contact and plastic zones just before failure.

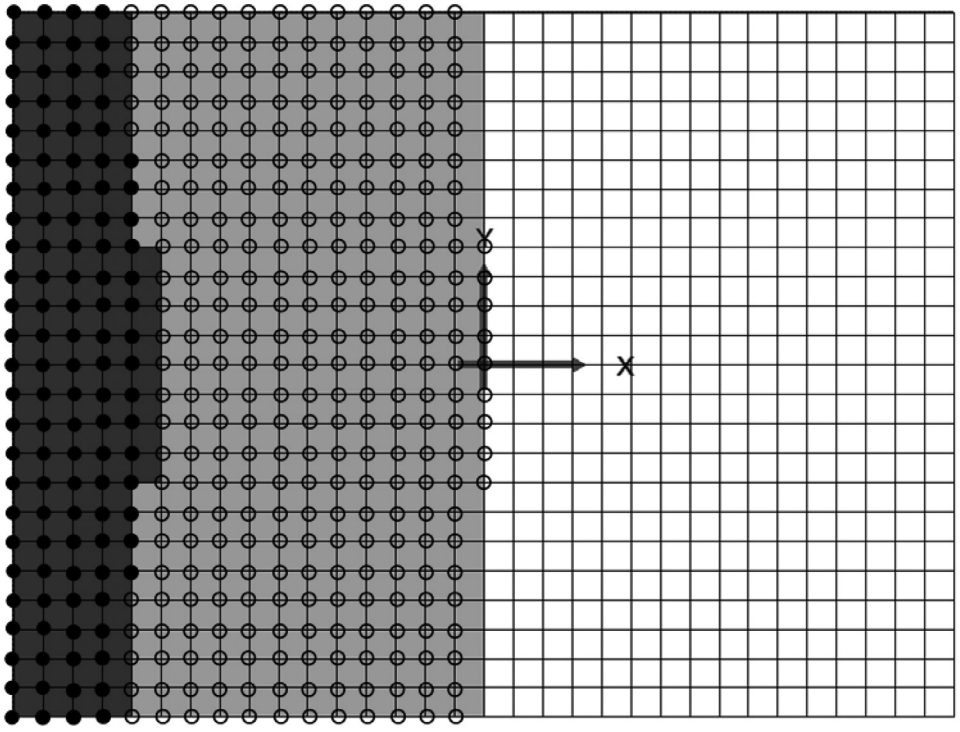

c: Contact and plastic zones for P= 0.65 MPa.

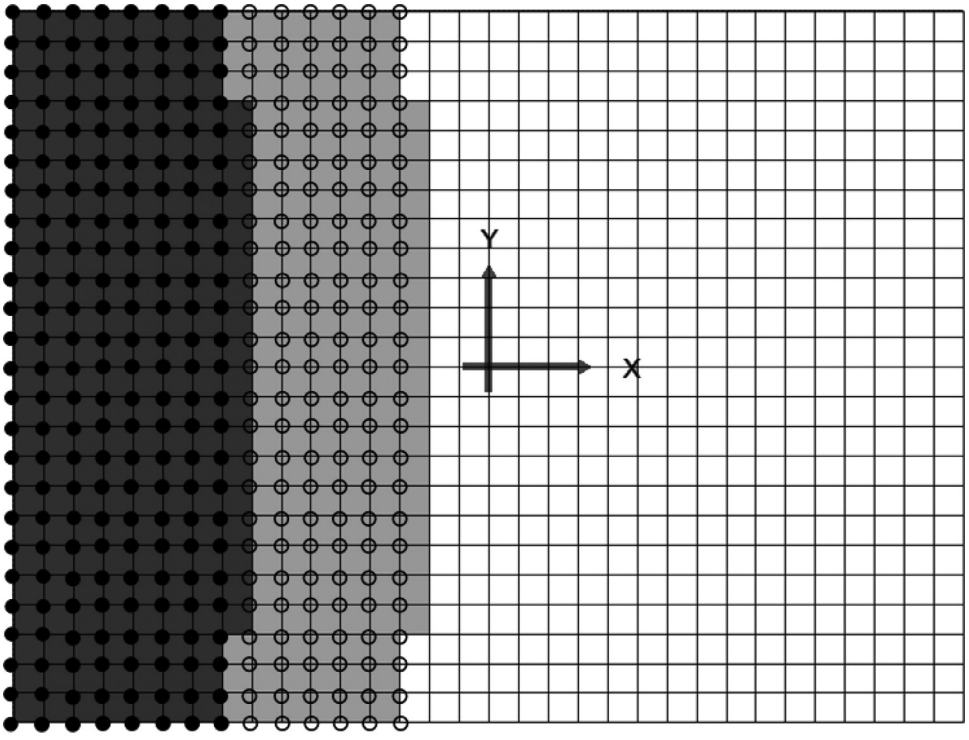

d: Contact and plastic zones for P= 0.7 MPa.

Fig. 34. Continued

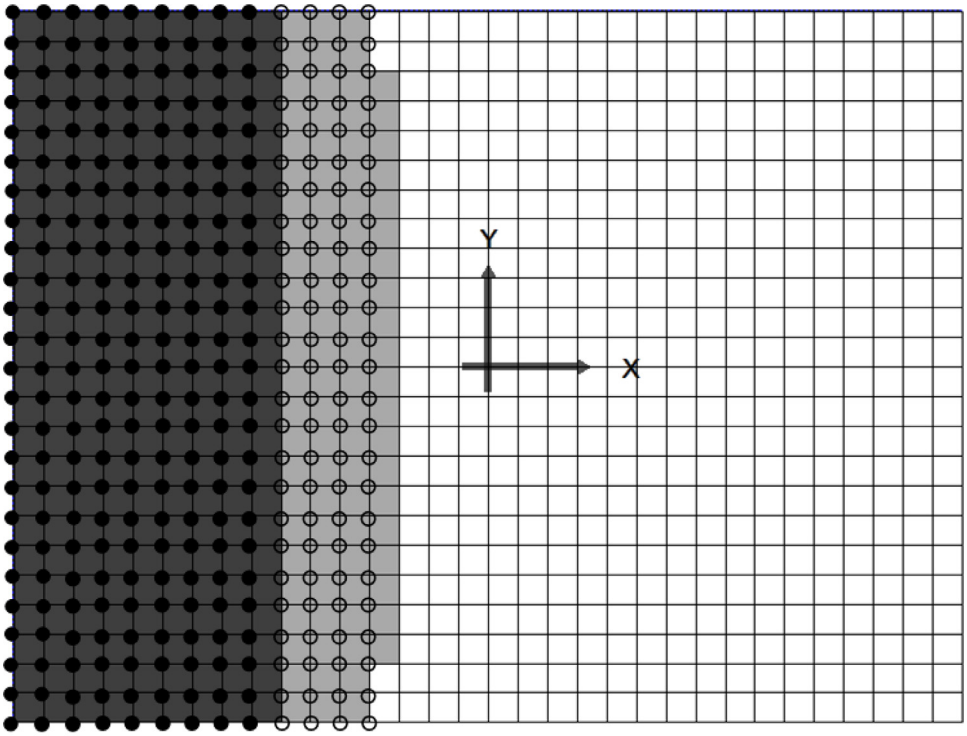

e: Contact and plastic zones for P= 0.71 MPa.

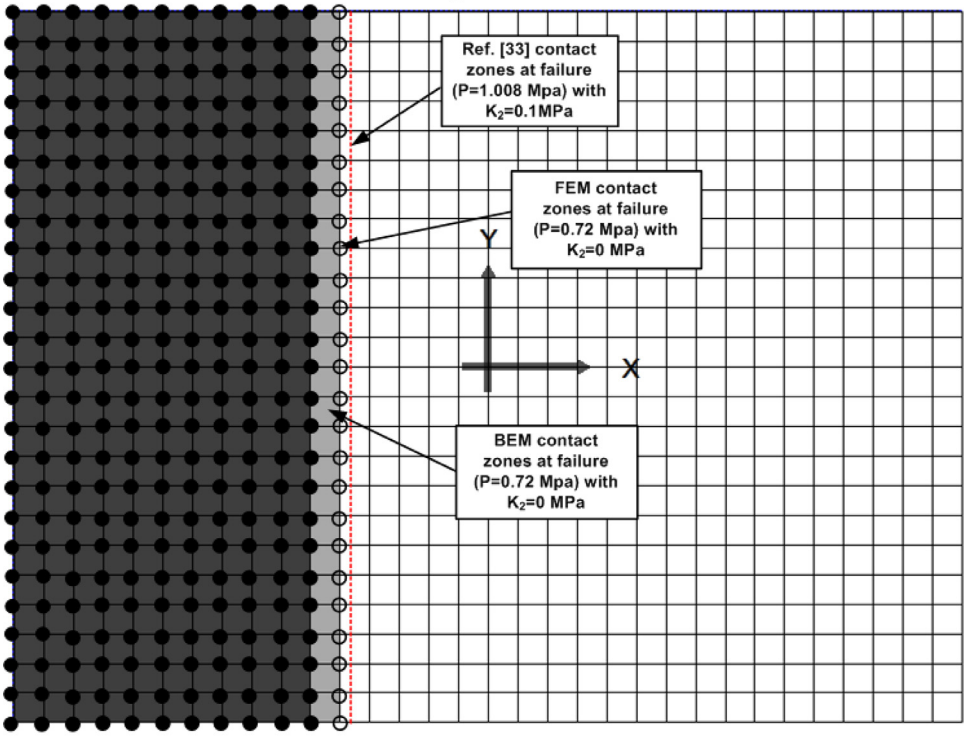

f: Contact and plastic zones just before failure.

Fig. 34. Continued

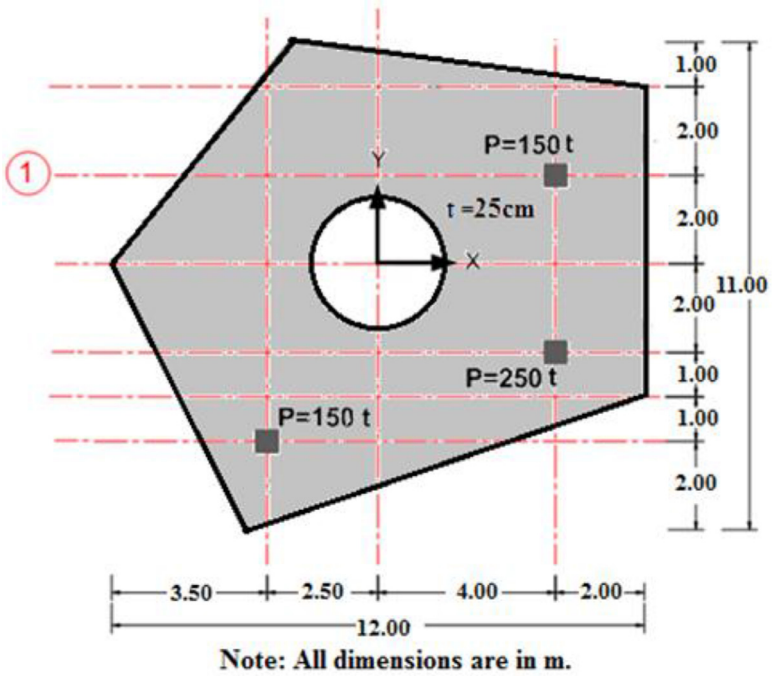

Fig. 35. The irregular plate considered in example 8.

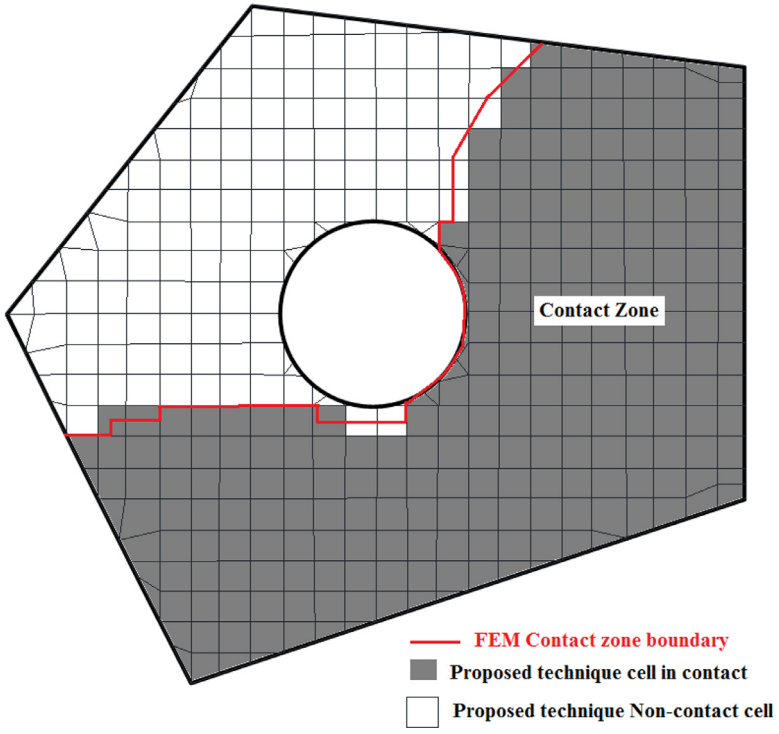

Fig. 36. The contact zones of the proposed technique and FEM model in example 8.

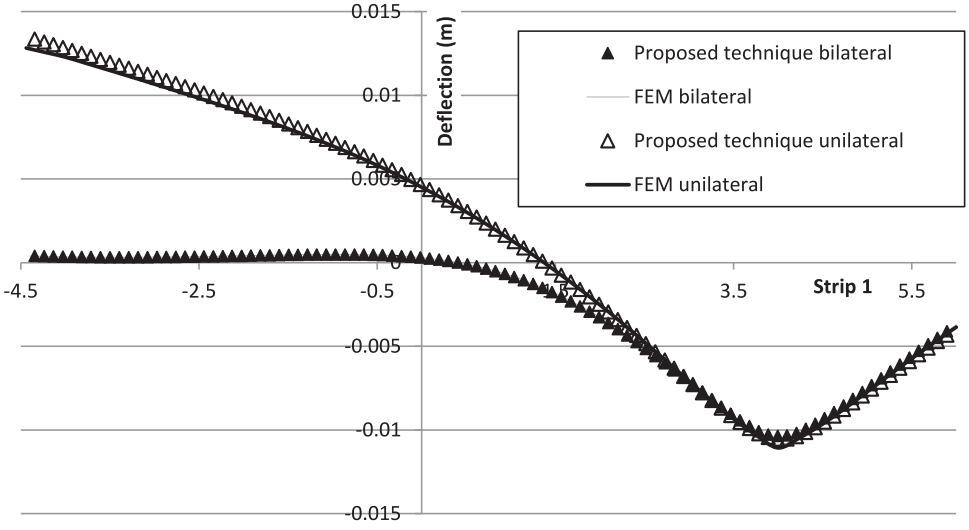

Fig. 37. Deflection along strip 1 for the irregular plate in example 8.

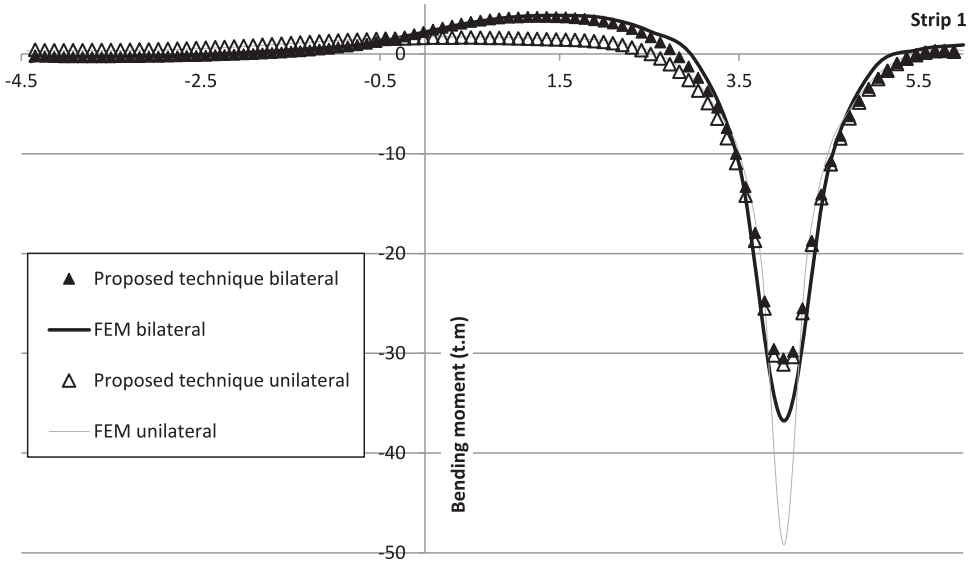

Fig. 38. Bending moments along strip 1 for the irregular plate in example 8.

Acknowledgments

This project was supported financially by the Science and Technology Development Fund (STDF), Egypt, grant no 14910. The first and third author would like to acknowledge the support of (STDF).

References

[1] Reissner E. On bending of elastic plates. Q Appl Math 1947;5:55–68.
[2] Cheung YK, Zienkiewicz OC. Plates and tanks on elastic foundations–an application of finite element method. Int J Solids Struct 1965;1:451–61.
[3] Svec OJ, McNeice GM. Finite element analysis of finite sized plates bonded to an elastic half space. Comput Methods Appl Mech Eng 1972;1:265–77.
[4] Svec OJ, Gladwel GM. A triangular plate bending element for contact problems. Int J Solids Struct 1973;9:435–46.
[5] Katsikadelis JT, Armenakas AE. Plates on elastic foundation by BIE method. J Eng Mech 1984;110:1086–105.
[6] Rajapakse RK, Selvadurai AP. On the performance of Mindlin plate elements in modeling plate-elastic medium interaction: a comparative study. Int J Numer Methods Eng 1986;23:1229–44.
[7] Syngellakis S, Bai SC. On the application of the boundary element method to plate-half space interaction. Eng Anal Boundary Elem 1993;12:119–25.
[8] Paiva JB, Butterfield R. Boundary element analysis of plate-soil interaction. Comput Struct 1997;64:319–28.
[9] Rashed YF, Aliabadi MH, Brebbia CA. The boundary element method for thick plates on a Winkler foundation. Int J Numer Methods Eng 1998;41:1435–62.
[10] Rashed YF, Aliabadi MH. Boundary element analysis of buildings foundation plates. Eng Anal Boundary Elem 2000;24:201–6.
[11] Rashed YF. A boundary/domain element method for analysis of building raft foundations. Eng Anal Boundary Elem 2005;29:859–77.
[12] Shaaban AM, Rashed YF. A coupled BEM-stiffness matrix approach for analysis of shear deformable plates on elastic half space. Eng Anal Boundary Elem 2013;37(4):699–707.
[13] Cheung YK, Nag DK. Plates and beams on elastic foundations-linear and nonlinear behavior. Geotechnique 1968;18:250–60.
[14] Weitsman Y. On the unbonded contact between plates and an elastic half-space. ASME J Appl Mech 1969;36:198–202.
[15] Weitsman Y. On foundations that react on compression only. ASME J Appl Mech 1970;37:1019–30.
[16] Svec OJ. The unbounded contact problem of a plate on the elastic half space. Comput Methods Appl Mech Eng 1974;3:105–13.
[17] Celep Z. Rectangular plates resting on tensionless elastic foundation. J Eng Mech 1988;114:2083–92.
[18] Li H, Dempsey JP. Unbonded contact of a square plate on an elastic half-space or a Winkler foundation. ASME J Appl Mech 1988;55:430–6.
[19] Hu C, Hartley GA. Analysis of a thin plate on an elastic half-space. Comput Struct 1994;52(2):227–35.
[20] Jirousek J, Zielínski AP, Wŕoblewski A. T–element analysis of plates on unilateral elastic Winkler–type foundation. Comput Assisted Mech Eng Sci 2001;8:343–58.
[21] Shen HS, Yu L. Nonlinear bending behavior of Reissner–Mindlin plates with free edges resting on tensionless elastic foundations. Int J Solids Struct 2004;41:4809–25.
[22] Torbacki W. Numerical analysis of beams on unilateral elastic foundation. Arch Mater Sci Eng 2009;29(2):109–12.

[23] Buczkowski R, Torbacki W. Finite element analysis of plate on layered tensionless foundations. Arch Civ Eng 2009;3.
[24] Kongtong P, Sukawat D. Coupled integral equations for uniformly loaded rectangular plates resting on unilateral supports. Int J Math Anal 2013;7:847–62.
[25] Sapountzakis EJ, Katsikadelis JT. Unilaterally supported plates on elastic foundations by the boundary element method. ASME J Appl Mech 1992;59:580–6.
[26] Kexin M, Suying F, Xiao JR. A BEM solution for plates on elastic half-space with unilateral contact. Eng Anal Boundary Elem 1999;23:189–94.
[27] Silva ARD, Silveira RAM, GonÇalves PB. Numerical methods for analysis of plates on tensionless elastic foundations. Int J Solids Struct 2001;38:2083–100.
[28] Xiao JR. Boundary element analysis of unilateral supported Reissner plates on elastic foundations. Comput Mech 2001;27:1–10.
[29] Silveira RAM, Pereira WLA, GonÇalves PB. Nonlinear analysis of structural elements under unilateral contact constrains by a Ritz type approach. Int J Solids Struct 2008;45:2629–50.
[30] Mindlin RD. Force at a point in the interior of a semi-infinite solid. Physics 1936;7:195–202.
[31] Bu XM, Yan ZD. Bending problems of rectangular thin plate with free edges laid on tensionless Winkler foundation. Appl Math Mech 1989;10:435–42.
[32] Bu XM, Yan ZD. Bending problems of rectangular Reissner plate with free edges laid on tensionless Winkler foundation. Appl Math Mech 1991;12:605–16.
[33] Lewandowski R, Switka R. Unilateral plate contact with the elastic-plastic Winkler–type foundation. Comput Struct 1991;39(6):641–51.